Spring 2011

Ultrasonic assisted layer-by-layer assembly for stable nanocolloids of Curcumin and Paclitaxel

Zhiguo Zheng

ULTRASONIC ASSISTED LAYER-BY-LAYER ASSEMBLY

FOR STABLE NANOCOLLOIDS OF

CURCUMIN AND PACLITAXEL

by

Zhiguo Zheng, M S

A Dissertation Presented in Partial Fulfillment
of the Requirements for the Degree
Doctor of Philosophy

COLLEGE OF ENGINEERING AND SCIENCE
LOUISIANA TECH UNIVERSITY

May 2011

UMI Number 3459742

UMI®

Dissertation Publishing

ProQuest®

LOUISIANA TECH UNIVERSITY

THE GRADUATE SCHOOL

April 7st 2011
_____
Date

We hereby recommend that the dissertation prepared under our supervision

by____Zhiguo____Zheng_____

entitled_____

" ULTRASONIC ASSISTED LAYER-BY-LAYER ASSEMBLY

FOR STABLE NANOCOLLOIDS OF CURCUMIN AND PACLITAXEL "

_____

_____

be accepted in partial fulfillment of the requirements for the Degree of

Doctor of Philosophy in Biomedical Engineering

_____
Supervisor of Dissertation Research

_____
Head of Department

Biomedical Engineering
_____
Department

Recommendation concurred in,

_____

_____   Advisory Committee

_____

Approved
_____
Director of Graduate Studies

Approved
_____
Dean of the Graduate School

_____
Dean of the College

ABSTRACT

Researchers have been trying to fight cancer with synthesis of new bioactive compounds but many of these novel drugs have low solubility in water and it is difficult to deliver them into a patient's body One way of solving this particular problem is to use nanoscale drug delivery systems In this dissertation, we describe using an ultrasonic assisted layer-by-layer encapsulation process to prepare anti-cancer drugs with 50~200 nm particle size with designed coating to achieve sustained release and target delivery

Two methods for systematic manufacture of low solubility anti-cancer drug nanoparticles were proposed 1) Top-down approach to breakdown larger drug crystals into nano-size particles 2) Bottom-up approach to fabricate nano size drug crystals from a drug solution

APPROVAL FOR SCHOLARLY DISSEMINATION

The author grants to the Prescott Memorial Library of Louisiana Tech University the right to reproduce, by appropriate methods, upon request, any or all portions of this Dissertation It is understood that "proper request" consists of the agreement, on the part of the requesting party, that said reproduction is for his personal use and that subsequent reproduction will not occur without written approval of the author of this Dissertation Further, any portions of the Dissertation used in books, papers, and other works must be appropriately referenced to this Dissertation

Finally, the author of this Dissertation reserves the right to publish freely, in the literature, at any time, any or all portions of this Dissertation

Author _____

Date 5/12/2011 _____

TABLE OF CONTENTS

VI

LIST OF FIGURES

LIST OF TABLES

ACKNOWLEDGMENTS

I would like to express my gratitude and appreciation to my advisor, Dr Yuri Lvov, for his guidance and suggestions all through this dissertation project I would also like to thank other members of my Advisory Committee and Dr Tanya Shutova for her friendly guidance

ABBREVIATIONS

BBB   Blood-Brain Barrier

BSA   Bovine Serum Albumin

DDS   Drug Delivery System

DLS   Dynamic Light Scattering

EDX   Energy Dispersive X-ray spectrometry

EPR   Enhanced Permeation and Retention

HPMA Hydrolyzed PolyMaleic Anhydride

LbL   Layer-by-layer

PAH   Poly(allylamine hydrochloride)

PEG   Poly(ethylene glycol)

PEI   Poly(ethylenimine)

PS   Protamine Sulfate

PSS   Poly(styrenesulfonate sodium)

PDDA Poly(dimethyldiallyl ammonium chloride)

QCM   Quartz Crystal Microbalance

QELS Quasi-Elastic Light scattering

SEM   Scanning Electron Microscope

XRD   X-Ray Diffraction

CHAPTER 1

INTRODUCTION

1 1 Motivation

Cancer is the second leading cause of death in the United States The National Cancer Institute estimated that 1,529,560 men and women (789,620 men and 739,940 women) will be diagnosed with, and 569,490 men and women will die from various of cancer in 2010 [1]

Researchers had been trying to fight cancer with new natural or synthetic bioactive compounds Although these novel compounds showed promising results in screening process, many of them exhibit low solubility in water because of the hydrophobic and/or polycyclic nature Low solubility often brings challenges to drug administration, because the traditional formulation usually cannot provide enough of the bioavailability required for treatment Also many of these compounds are highly toxic to normal cells so targeted delivery of the drug to the tumor tissues is required One way of solving the problem is to establish a drug delivery system that uses nano size drug particles with appropriate coating Our project will use an ultrasonic assisted layer-by-layer encapsulation process to prepare anti-cancer drug with 50~200 nm size with a designed coating to achieve sustained release and targeted delivery

1.2 Outlines

1.2.1 Objectives of the study

We developed the following directions in our work

1 We will systemically establish a process to fabricate nano size, low solubility

   drug particles (paclitaxel and curcumin)

2 We will optimize the process established in 1 to reduce the drug particle size

3 We will compare different layer-by-layer coatings for sustained release

1.2.2 Outline of the dissertation

This dissertation is arranged into eight chapters Chapter 1 provides an

introduction to the dissertation by describing the motivation and purpose of the study as

well as the outline of the dissertation Chapter 2 is the literature review, in which we

will discuss nanoscale drug delivery systems in general and compare different types of

existing nanoscale drug delivery systems This is followed by a short introduction to the

layer-by-layer self-assembly coating drug delivery system In Chapter 3, we introduc

the material, instruments, and general methods that were used in this research Chapter

4 is focused on the top down approach which breaks down big drug particles into nano

size particles Chapter 5 will show a different bottom up approach which forms nano

crystals from solution using ultrasound Chapter 6 will optimize particle size by

changing various parameters, like sonication time and concentration Chapter 7 will

study the release profile of different nano drug particles The main accomplishments of

the dissertation work are summarized in Chapter 8, with directions for further research

CHAPTER 2

NANOSCALE DRUG DELIVERY SYSTEM

2.1 Nanoscale Drug Delivery System

With the application of nanotechnologies to medicine, a new branch of nanotechnology, called nanomedicine, has been rapidly developed [2] Nanoscale drug delivery systems use nanosize drug carriers to deliver drugs to the desired sites And often use active or passive targeting strategies to increase local concentration at the tumor tissue [3]

Goals of a nanoscale drug delivery system include

1 Improved solubility To increase the drug bioavailability

2 Targeting To increase the local concentration of the drug at desired sites

3 Adjustable rate of drug release To maintain a constant dose at the action site

4 Reduced drug clearances To increase the drug half-life

5 Enhanced stability To reduce drug degradation during storage

6 Drug delivery across biobarriers like the blood-brain barrier (BBB)

The goals of the drug delivery system were to deliver the conjugated or bound drug-carrier complex to the selected target and maximize act at desired cancer sites Controlled delivery of the drug molecules using carrier materials are based on two types of strategies active and passive targeting Although the former has very sophisticated strategies, its practical use still suffers from many technical difficulties The latter is

3

more practical, and there are already many formulations based on "enhanced permeability and retention effect" [4, 5], which has been the most representative passive-targeting strategy to bring drug molecules to tumors

The active targeting strategy of the drug nanocarrier was to use a ligand, attached on the nanocarrier, specific for the receptor of the target tissue Passive targeting strategy of the drug nanocarrier was to use the enhanced permeation and retention (EPR) effect of the cancer tissue Tumor and inflamed tissue tend to have excessively leaky microvasculature, compared to normal endothelium, which allows the drug nanocarrier to diffuse through and accumulate at site Especially for cancer tissue, overexpression of vascular endothelial growth factor will increase vascular permeability and let to complicated tumor-vessel architecture Transvasation of durg carrier takes place either via transcytosis, where by macromolecules are internalized from the blood at points of invagination of the cell membrane, or paracellularly, via diffusion through the tight junctions of endothelial cells In combination, these effects cause enhanced permeation and retention (EPR), resulting in high local drug concentrations

For nanoscale drug delivery systems, biocompatibility and biodegradability have always been considered as one of the most important properties The unloaded carrier should be able to biodegrade or metabolize into nontoxic components and cleared through the circulation system Some studies suggested nanoparticles are cleared according to size Small particles (<30 nm) are rapidly cleared by renal excretion Nanocarriers >30 nm are cleared by the mononuclear phagocytic system, consisting of macrophages located in the liver (Kupffer cells) and the spleen [6], which act as phagocytotic scavengers Clearance is also dependent on the endothelial fenestral pore

size [6] Fenestral pore size values are highly variable for different patients Clearance rate of patient could be effect by sex, age and genetics factors It is difficult to determine the efficiency and toxicity of nanomedicines in different individuals Whether nanocarriers are taken up by macrophages depends on opsonization by the innate immune system [7] Molecules that bind to foreign materials and enhance phagocytosis, include IgG and IgA antibodies, the complement cascade system and mannose-binding lectin [8] Therefore, the surface properties of nanocarriers can significantly affect the rate of clearance by the MPS A useful method for evading opsonization of large narrow carriers was developed at Rutgers University [9] in a process call PEGylation, a polymer, poly(ethylene glycol) (PEG, $[CH_2CH_2O]_n$), is conjugated to the drug carrier preventing drug particles aggregation and precipitation

Overall, the use of ligand binding nanodrugcarrier will improve the drug therapeutic index according to Equation (1)

$$\text{Therapeutic index} = \frac{\text{Maximum non - toxic dose}}{\text{Minimum effective dose}}$$ (Eq 1)

The high specificity and selectivity of the ligand on nanodrugcarrier increases the amount of drug delivered to the cancer tissue and decreases the amount of drug at unwanted sites Therefore, a less systemic drug dose needs to be administered to guarantee an effective concentration at the site of action, and the minimum efficacious dose is also lower In addition, because less drug is present at unwanted sites, the maximum non-toxic dose is higher The overall effect is a significant decrease in toxicity and adverse side effects

2.2 Current Nanoscale Drug Delivery System

Nanoscale drug delivery systems can use different kind of nanoparticles as carriers In this section we will review some of the most common category of nanoparticles can be used as drug delivery systems Figure 2-1 shows the structure schematics of these nanoparticles
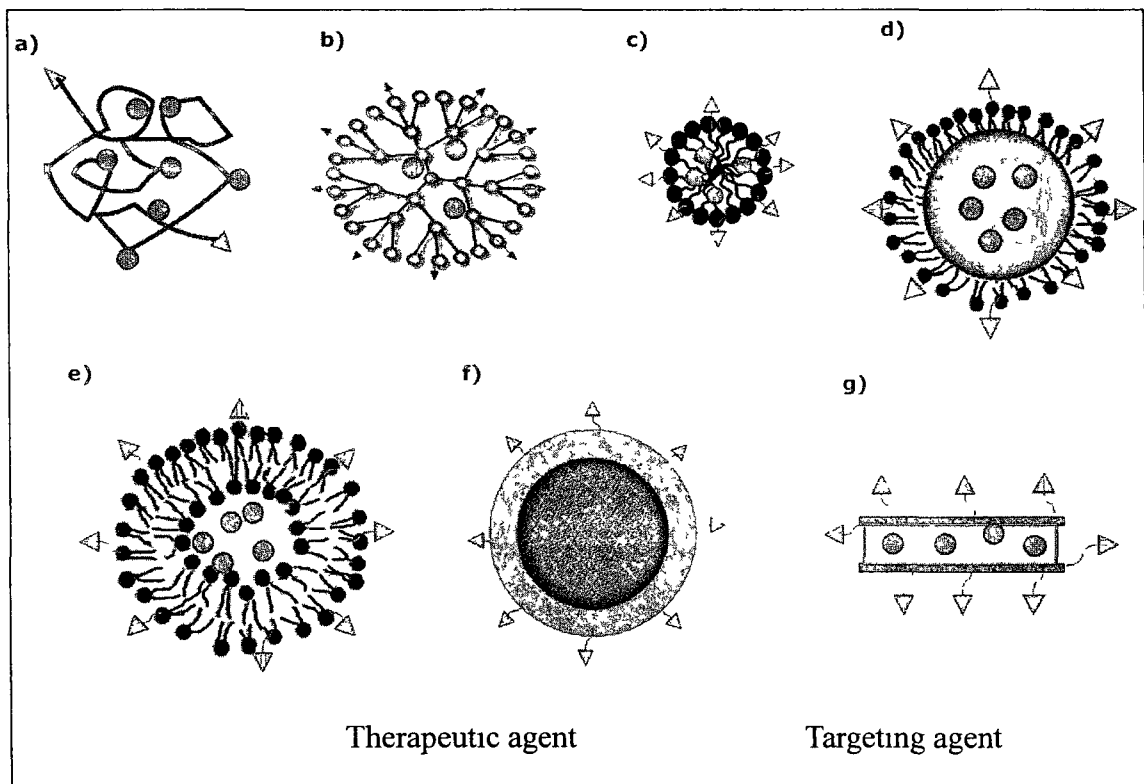
Figure 2-1 Classification of nanoscale drug delivery System
a) drug conjugate, b) dendrimer, c) micelle,
d) microemulsion, e) vesicle, f) core-shell nanoparticle,
g) nanotube

2 2 1 Drug complex and conjugate

Drug complexes and conjugates do not have a defined structure like micelle or vesicle Drug complexes depend on reversible interactions between carrier and drug

Drug conjugates use covalent bonds to join carrier and drug together [10] Drug conjugates can be prepared using chemical reactions of functional groups between the drug and the carrier molecular There are two major categories of drug complexes and conjugates one is protein and peptide associated and the other is polymer associated Proteins and peptides can be used to form nano structures in various ways, including complexation An example of protein associated drug complex nanoparticle for clinical use is Abraxane[TM] Abraxane[TM] is an albumin-bound form of paclitaxel with a mean particle size of approximately 130 nanometers Paclitaxel exists in the albumin-bound particles in a non-crystalline form Abraxane[TM] is formed by dissolving paclitaxel in water immiscible methylene chloride, and adding this to a solution of human serum albumin in water with low-speed homogenization This process creates an emulsion with albumin located at the aqueous-solvent interface Subsequent high-pressure homogenization reduces the particle size and breaks and reforms the disulfide bonds, essentially crosslinking the albumin coating and stabilizing the particle An evaporation step volatilizes the methylene chloride, leaving an aqueous suspension of 140-160 nm nanoparticles, consisting of an amorphous paclitaxel core surrounded by a 25 nm coating of albumin with bound paclitaxel Because of its size this material can be sterile filtered [11, 12] Abraxane[TM] does not contain the problematic solvent - Cremophor EL, which outperformed conventional paclitaxel at an equitoxic dose while decreasing toxicity, due to longer circulation time and lower off-target activity [13, 14] Supramolecular complexes between host and guest molecules are also considered as useful for the drug administration Cyclodextrins are natural products and can entrap entire or part of guest drugs in their inside cavity in a specific mode Chemical modification of natural cyclodextrins molecular could improve their efficacy by altering

their solubility or capacity for the guest drugs Cyclodextrins are regarded as useful additive in drug delivery systems [15, 16]

2.2.2 Dendrimer

Polymeric dendrimer is a kind of hyperbranched nanostructures One of dendrimers' advantages is that its size can be controlled by adjusting the number of polymerization generations During the polymerization progcess, monomer molecules joined into a spherical nanostructure Inside this dendrimer nanostructure are cavities which allowed therapeutic agents to be loaded with great loading efficiency [17]

The polymerization progresses of dendrimers can be precisely controlled to obtain the desired final product The molecular weight, chemical composition, and nanostructure of the final product can be precisely designed [18] With controlled polymer structure and narrow polydispersity, dendrimers may be ideal platforms for drug delivery system An example of dendrimers for clinical usage is VivaGel [TM] It is currently on trial for safety and efficacy as a microbicide

2.2.3 Micelles

Micelles are one of the simplest molecular assemblies and can carry hydrophobic drugs in their central core or in their palisade layer [19] Micelles nanoparticles are interesting structures for carriers of drugs because they can form relatively uniform size structures Micelles can be formed using a variety of amphiphilic materials as outside coating and using hydrophobic drug as central core, and can incorporate multiple functionalities into a single structure Unfortunately, surfactants used to form micelles often have toxic effects on human bodies Only a few kinds of surfactant are approved by FDA for drug solubilization Additional use of organic solvents may increase drug solubility but disturbs micelle formation in some cases [20,

21] Lacking an aqueous core, the drug must be bound to the polymer before micelles formation Drug needs to be conjugated to an anchor polymer molecule, or entrapped and bonded inside the hydrophobic core of the micelle [22] Micellar structures, including polymeric micelles, have been extensively studied as drug carriers [23] Polymeric micelles made of hydrophilic-hydrophobic block copolymers are used as drug carriers [34] which can be concentrated in the tumor tissue based on the EPR effect [25], and may be used for gene therapy as well [26] Because hydrophilic-hydrophobic block copolymers' critical micelle concentrations are much lower than those for low-molecular-weight surfactants, they have higher stability and lower toxicity The hydrophobic portion of the copolymer forms the micellar core The hydrophilic block of the copolymer forms the micellar corona This corona (commonly consisting of PEG, HPMA, or other hydrophilic polymers) confers these micelles with biocompatibility, stealth-like properties, and a platform for functionalization [27-29] Genexol-PM^{TM} is a formulation of paclitaxel encapsulated in a polymeric micelle formed by the solid dispersion technique from the biodegradable block copolymer, monomethoxy poly(ethylene glycol)-block-poly(D,L-lactide) [30] Several clinical trials have already been carried out evaluating the safety and efficacy of Genexol-PM^{TM} in metastatic breast cancer, solid tumors, and non-small-cell lung cancer [31-33]

2.2 4 Microemulsion

Entrapment of drugs within emulsions [34] results in various improvements in the performance of the drugs including suppression of side effects, prolonged drug retention in blood circulation, and enhanced drug efficacy at the target site based on the EPR effect Lipid emulsions have a long history in the pharmaceutical practice as nutrients, commercialized emulsion formulation was achieved relatively easily by

incorporating hydrophobic drugs, such as steroids, into the traditional emulsions Microemulsion is an equilibrated solution, unlike emulsions, and it is utilized for oral formulations [35-37] Formulations containing surfactants, drugs, and oils, which were designed to spontaneously form microemulsions upon contact with water in the stomach and small intestine, induce reproducible drug release This formulation offers great contribution to organ transplantation [38], since it requires precise control of the immunosuppressant concentration in plasma Microspheres composed of appropriate polymers, such as biodegradable polymers, enable prolonged drug-release after intravenous injection Administration frequency has decreased from daily to monthly by using this carrier [39]

2.2.5 Vesicles

Vesicular structures have been extensively studied as drug delivery system The two major categories of vesicles are liposomes and polymer vesicles Vesicles have the capacity for encapsulation of hydrophobic or hydrophilic drugs Vesicles can be design to use covalent or non-covalent bonds to load drugs Liposomes, (or lipid vesicles) [40] can be used to load hydrophilic drugs into an interior aqueous phase Liposomes can also be used to load hydrophobic drug lipid phase in the shell Liposomes are considered to be ideal drug carriers, because of their surface characteristics can be altered easily and their size is controllable Use of liposomes as a clinical drug delivery system still need to face some technical difficulties like mass production, storage stabilities, and lack of efficacy after accumulating a the target site Recently, liposomes have also been studied as non-virus vectors for gene therapy [41] Liposome formulations for drug delivery have been in development for almost half a century, and have produced clinically successful applications [42] Polymeric vesicle structures, or

polymersomes, have been described more recently, and have unique potential as drug carriers An example of the clinical vesicle formulation is Doxil ™, also known as liposomal Dox Encapsulation of Doxorubicin in liposomes shielded by polyethylene glycol (PEG) prolongs systemic drug circulation, improves safety, and increase the therapeutic index relative to free Doxorubicin [44, 45]

2.2.6 Core-shell nanoparticles

Core-shell structured nanoparticles consist of an inner nanoparticle core and a hydrophilic shell The inner nanoparticle core could be made with a wide variety of materials including Quantum-dots, metals, metal oxides, and polymers among other materials The core is surrounded by a hydrophilic shell usually using covalent or ionic bonds or electrostatic force

One category of core-shell nanoparticles has been developed during the chemical modification of gold and other materials nanoparticles to increase their physiological stability and control drug association and release [46] These core-shell nanoparticles offer stability and modifiable surface properties, and can even produce contrast depending on their composition, size, and shape [47, 48] These core-shell structured nanoparticles make for a very robust drug delivery vehicle due to the vast variety of elements that can be used as the core and shell components Despite the advantages already mentioned, these core-shell nanoparticles suffer from some inherent shortcomings, such as biotoxicity, rapid clearance rate, and poor biodistribution and biodegradation Various strategies are in development to circumvent these problems [49, 50]

Another category of core-shell nanoparticles uses porous materials as an inner core to carry drug Porous materials with large surface area and pore volume are

regarded as good candidates for drug storage and delivery As a example, mesoporous silica have been investigated as a drug carrier materials because of its mesochannels, which have defined diameters in the ranges of nanometers to tens of nanometers provide reliable nanospaces for drug accommodations [51, 52] In addition, their huge pore volume per unit mass of materials enables us to entrap large amounts of drugs In some pioneering approaches, the inlets of channels are modified to add gate functions, resulting in controlled release by external stimuli [51-53] Not limited to mesoporous silica, mesoporous carbon and related materials [54, 55], biocompatible porous calcium phosphate [56], and metal-organic frameworks (MOF) [57] have also been paid attention as future strong candidates for drug delivery applications

2.2 7 Nanotubes

Carbon nanotubes are used as drug carriers because of their nanocavities and high surface area [58, 59] However, there is much concern regarding the long-term toxicity of the nanotubes in practical uses due to their geometrical similarity to asbestos [60] Carbon nanohorns may be a better candidate for drug carrier [61] due to theirs lower aspect ratio, which is considered to play important role in the toxicity Carbon nanotubes (CNTs) are cylindrical tubes composed solely of carbon and can be formed either as single-walled or multi-walled, for more stability [62] These CNTs are being investigated as therapeutic nanoparticles because of their tunable properties and ability to incorporate multiple functionalities Amine-functionalized, single-walled CNTs were conjugated by amide-linking to a cisplatin-folic acid derivative as targeted delivery system, has show better performence than a conventional cisplatin formulation [63]

Another study conducted by Rusling et al used carboxylated single-walled CNTs conjugated with cisplatin and epidermal growth factor to target cancer cells

which have overexpress of the epidermal growth factor receptor The targeted CNT-cisplatin conjugate improved the selective killing of the targeted tumor cells [64] Many studies have reported CNTs to be effective carriers of therapeutics and imaging agents *in vitro*, however, *in vivo* studies have lead to concerns regarding the associated toxicities [65-67]

An interesting development was recently reported on drug delivery with halloysite clay nanotubes [68-71] These clay nanotubes have a larger diameter than carbon nanotubes (ca 50 nm external diameter, 15 nm lumen diameter and length of ca 800 nm), and they are biocompatible [72] Drugs may be loaded into these tubes within a minute at ca 10-20 wt % and then slowly released over 10-50 hours [69] It is not assumed that it would be possible to inject halloysite clay nanotubes into the blood stream, due to their inorganic composition, but their applications for dermatological (including rectal), cosmetic and dental delivery were considered as well as incorporation into bone and tooth implants

2.3 Layer-by-layer Coated Nanoparticles for Drug Delivery

2.3.1 Outline of LbL assembly

Before we discuss the LbL capsules for drug delivery we will first briefly review the layer by layer self assembly technique in this section [73, 74] Self-assembly of the nano particles using electrostatic interactions through a layer-by-layer process, was first proposed by R K Iler [75] The idea was developed and first realized by Decher, Mohwald, Lvov, et al [76, 77] Because the self assembling mechanism is so simple, the requirements for the apparatus necessary for the process are very low (requiring only beakers and tweezers) [78], and the procedures are easy to perform, this methodology was quickly adapted by many research groups with the utilization of layer by layer

assemblies of various materials including synthetic polymers [79-80], biomaterials [81-84], inorganic materials [85-87], and supra-molecular assemblies [88-90] Relatively high concentrations of the charged substances in the solution results in excess adsorption of the substances The surface charge was first neutralized and then resaturated lead to charge reversal (Figure 2-2) Reversing of the surface charge makes a continuous assembly between positively and negatively charged materials The driving forces for the LbL self-assemblies are not limited to electrostatic interactions Many kinds of interactions , such as metal coordination [91, 92], hydrogen bonding [93, 94], covalent bonding [95, 96], supramolecular inclusion [97], bio-specific recognition [98, 99], charge transfer complex formation [100], and stereo-complex formation [101, 102] were reported and could be used in the LbL process Many other deposition techniques including spin-coating [103, 104] and spraying [105], were used for the LbL assembly Also automatic machines were developed for the LbL assembly [106, 107] The materials used for LbL assembly also have been widely tested In the 90's, most researchers used synthetic polyelectrolytes, such as PAH, PEI, PDDA, PSS and PAA, but current research, especially related to biomaterials and pharmacology, uses natural biodegradable polyelectrolytes, including positively charged chitosan, dextran amine, gelatin A, protamine sulfate, and negatively charged chondroitin sulfate, dextran sulfate, hyaluronic acid, heparin, gelatin B and sodium alginate
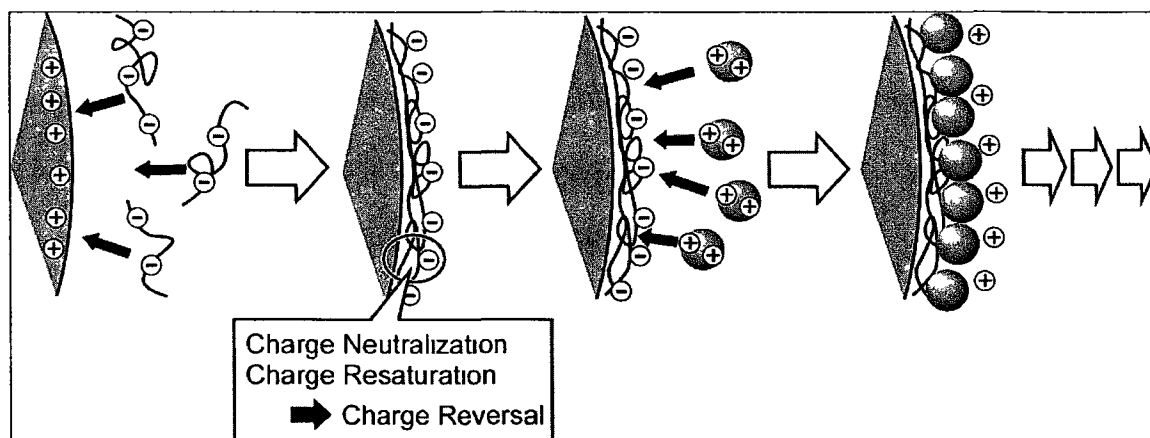
Figure 2-2 LbL assembly process outline

The LbL assembly techniques are considered suitable for biomaterials, because the process is simple and is performed in mild environment The LbL assembly is usually performed at room temperature in a pH neutral aqueous solution Because the LbL technique does not require special conditions like high temperature or extreme pH, biomaterials can be assembled under favorable conditions Another advantage of the LbL assemblies for biomaterials is the porous nature Unlike Langmuir-Blodgett (LB) films, LbL films allow diffusion of materials Activities of the enzyme glucose oxidase were reported to be blocked after covering with only a few layers of lipid LB films [108, 109] The LbL films with a single component enzyme (glucose oxidase) or multiple enzymes (glucose oxidase and glucoamylase) do not have a serious decrease in enzyme activity after an increase in the numbers of layers [110, 111] These facts show that LbL films allow the diffusion of materials This ability is a crucial factor in drug delivery functions Additionally, it was also reported that biomaterials embedded within the LbL films show better stabilities [112]

An important development in the LbL technique was applying LbL technique to assembly on colloidal particles [113] This technique was first developed by G Sukhorukov, E Donath, F Caruso, and H Mohwald in the Max Planck Institute for Colloids and Interfaces [113-122], and then was quickly adapted by other groups

Instead of using conventional flat surface supports, LbL films were assembled sequentially on a colloidal core Subsequent destruction of the central colloid particle core could lead to hollow shells A typical example of preparing functional hollow shells is shown in Figure 2-3 where DNA molecules, retaining the natural double-helix structure, were encapsulated inside a biocompatible polyelectrolyte microshell [123, 124] In the first step, $MnCO_3$ particles were used as template, cores were suspended in a DNA solution, and the addition of spermidine solution into stirred $MnCO_3$/DNA solution caused precipitation of a water-insoluble DNA/spermidine complex onto the $MnCO_3$ particle Then in the second step, LbL assemblies of biocompatible polyarginine and chondroitin sulfate on the complex core were conducted In the third step, dissolution of the $MnCO_3$ template particles resulted in biocompatible shells containing a DNA/spermidine complex In addition, further decomposition of the DNA/spermidine complex led to a selective release of low molecular weight spermidine to complete the DNA entrapment In another example, De Smedt and coworkers reported a labeling system for LbL drug delivery using the barcode concept with encoded fluorescent polystyrene with captured antibodies [124]
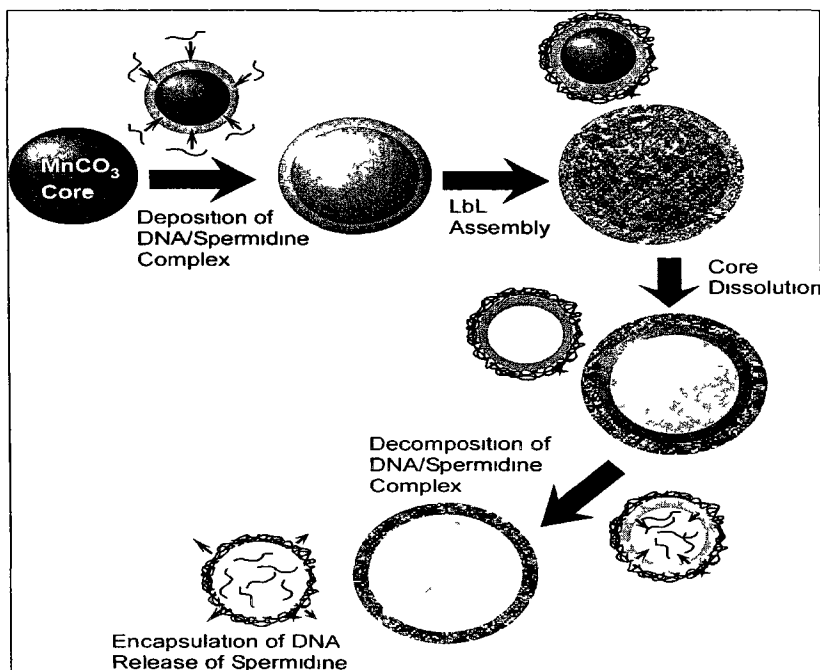
Figure 2-3 Preparation of functional hollow shells

2 3.2 Recent progress of LbL microshells in drug delivery functions

The LbL microshells could be used in many applications including in life science [125-127] The LbL microsells used as drug carriers have been attracting a lot of attention Most LbL shells used in these applications have diameter at micrometer range Raichur et al reported encapsulation and release profiles of rifampicin, an antituberculosis drug, using hydrogen-bond assembly LbL microshells of poly(vinyl pyrrolidone) and poly(methacrylic acid) [128] Release profiles showed a burst release Above pH 7, the maximum release rate was achieved because the microshells rapidly disintegrate The rifampicin released from the LbL microshells shows the same efficacy as the free drug This result indicates the drug properties have not changed because of possible disturbances during the encapsulation and release process Zhao, et al reported the loading of doxorubicin, an anti-tumor drug, into preformed LbL microshells The doxorubicin loaded LbL microsells' effect in tumor treatment was assayed by *in vitro*

cell culture tests and *in vivo* animal experiments [129] The LbL microshells contain negatively charged carboxylmethyl cellulose which entraps levels of the positively charged doxorubicin ten to a hundred times higher than the feeding concentration The encapsulated doxorubicin can effectively trigger the apoptosis of HepG2 tumor cells on *in vitro* tests The result shows that the LbL microshells have the ability for drug delivery and cancer treatment on an animal experimental level Chen, et al encapsulated another anti-cancer drug artemisinin in the crystal form with LbL microshell containing chitosan, gelatin, and alginate using LbL technique [130] The release rate of artemisinin could be adjusted by various parameters, such as polyelectrolyte types, number of polyelectrolyte layers, sodium chloride concentration, and ethanol concentration in the polyelectrolyte solution

Many researchers also try to control of drug release using external stimulaton Zhang, Gu, et al synthesized alginate-templated magnetically sensitive LbL microshells [131] When a high-frequency magnetic field was applied, doxorubicin's drug release rate from the microshells was significantly increased The doxorubicin-loaded microshells showed much lower cytotoxicity at the high drug concentration in comparison with doxorubicin Choi et al prepared LbL microshells containing photoacid generators, which made them UV sensitive [132] UV light will induce activation of photoacid generators and lead to the release of protons The decrease in the pH of the solution triggered the swelling of the LbL microshells Thus, opening and closure of the LbL microsell was achieved by exposure to UV light and washing with pH neutral water In addition, prolonged UV light exposure led to the breakage of the LbL microshells, which results in rapid release of the entrapped drugs

Protein delivery using LbL shells is also an active area in current research Zhang, Li, et al reported encapsulation and controlled release of protein using biodegradable LbL microshells The microshells consisted of dextran sulfate and chitosan Bovine serum albumin (BSA) was used as the model protein BSA was encapsulated in the LbL shells [133] The cell viability test indicated that the LbL microshells had good biocompatibility De Geest, Parak, et al encapsulated with a model of a nonactive prodrug, a self-quenched fluorescence-labeled protein in biodegradable LbL microshells [134] After the microshells uptake by living cells, the walls of the microshells were degraded and digested by intracellular proteases Wall degradation allowed intracellular proteases to reach the protein loaded inside of the microshells Enzymatic fragmentation of the fluorescence-labeled protein leads to individual fluorescence-labeled peptides So, only prodrugs inside the microshells that reach into the cells are the only ones activated, and those in shells in the extracellular environment cannot be activated Akashi et al reported entrapped proteins inside biodegradable microshells via LbL assembly Chitosan and dextran sulfate were assembled onto a protein-entrapping mesoporous silica particles, and then the silica was subsequent dissolved [135] Sustained release of the encapsulated proteins was achieved by using the enzyme to degrade the hollow shells

Variously specifically designed polymers have been used to compose the LbL microshells For example, Vancso et al developed organometallic polyelectrolyte multilayer microshells, which are composed of polyanions and polycations of poly(ferrocenylsilane) (Figure 2-4) [136] Poly(ferrocenylsilane) have redox-active ferrocene units in the main chain, which makes the shell wall permeability sensitive to the redox state In fact, the permeability of these microshells can be tuned using

chemical oxidation, resulting in a fast shell expansion accompanied by a significant

permeability increase in response to a very small trigger
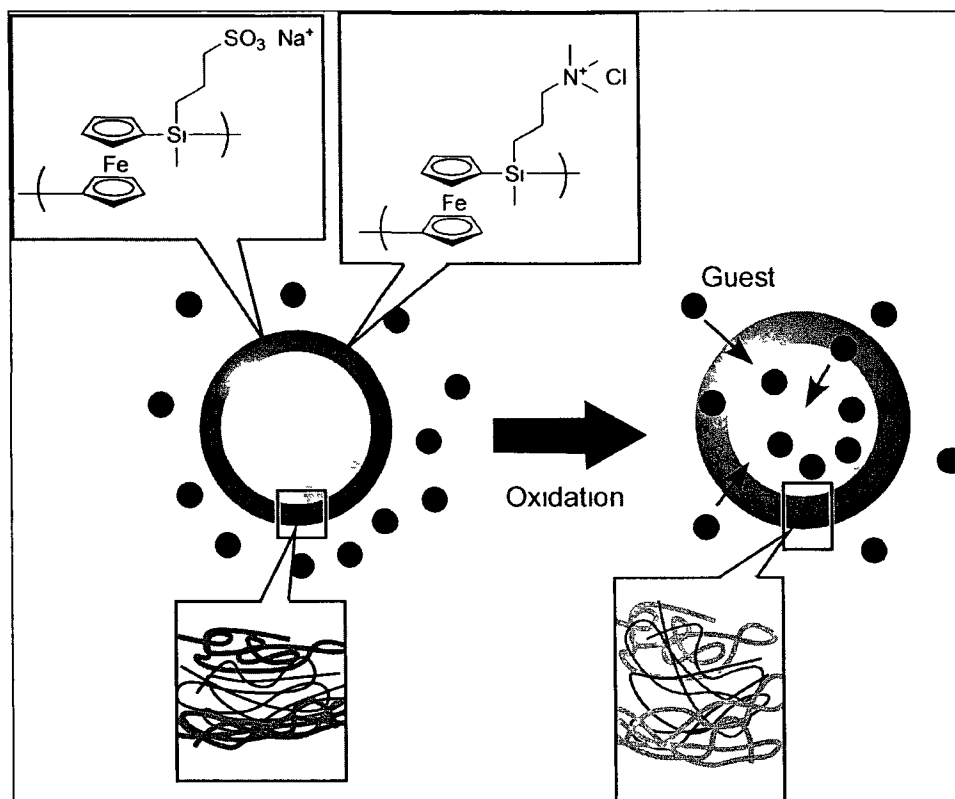
Figure 2-4 Organometallic polyelectrolyte multilayer microshells,
composed of polyanions and polycations of
poly(ferrocenylsilane)

Caruso et al developed a new type of polymer hydrogel LbL microshells based

on disulfide cross-linked poly(methacrylic acid) and poly(vinylpyrrolidone) The

disulfide cross-linking is sensitive to redox state It can act as redox-active trigger for

shell degradation [137] They also developed degradable LbL microshells as drug

carriers for the delivery of oligopeptide antigens to antigen presenting cells (Figure 2-5)

[138] Oligopeptide sequences were first covalently linked to a negatively charged

polymer via biodegradable linkages Then this conjugate was adsorbed onto amine-

functionalized silica particles The peptide-coated particle was coated with thiolated poly(methacrylic acid) (PMA$_{SH}$) and poly(vinylpyrrolidone) (PVPON) Dissolving of the silica core and disruption of the hydrogen bonding between polymers resulted in disulfide-stabilized microshells Glutathione, a natural reducing agent, can be used to cut the disulfide bonds which causes release of the peptide from the microshells
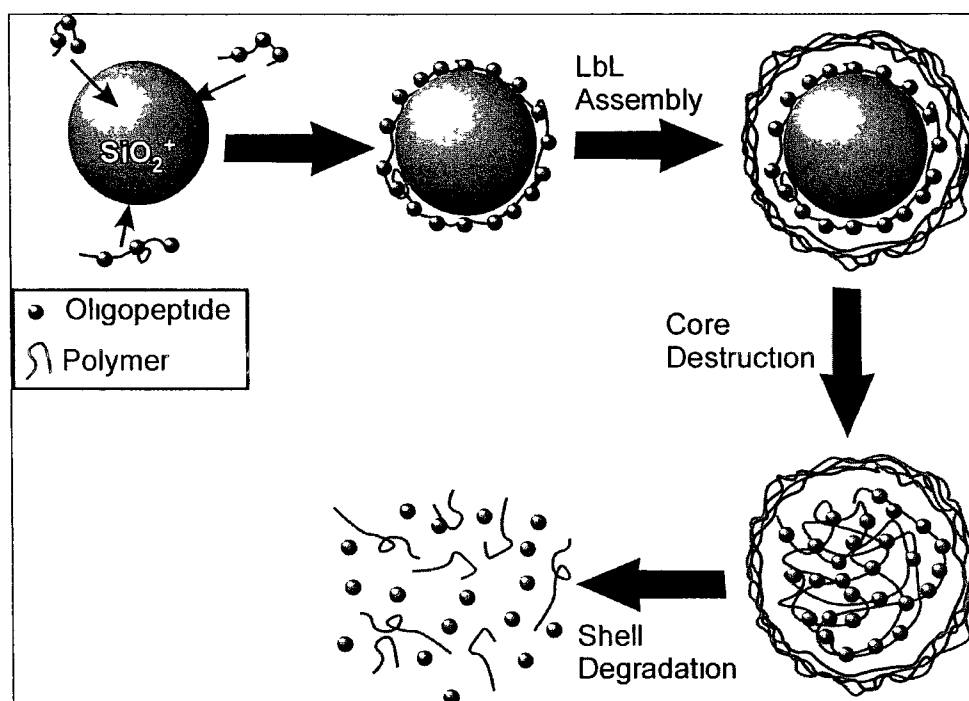
Figure 2-5 Degradable polymer microshells as carriers for the delivery of oligopeptide antigens

Many researchers combine of the LbL technique with other molecular assembly technique, such as liposomes or micelles, together to create various shell systems Addison et al develpoed LbL microshells constructed entirely from a cationic/ zwitterionic pair of pH-responsive block copolymer micelles [139] Layers of anionic poly[2-(dimethylamino)ethyl methacrylate-block-poly(2-(diethylamino)ethyl metha-crylate)] and cationic poly(2-(diethylamino)ethyl) methacrylate-block-poly(meth-

acrylic acid) copolymer micelles were alternately assembled onto $CaCO_3$ colloidal templates Then add in dilute ethylenediaminetetraacetic acid solution to dissolve the $CaCO_3$ core and form hollow polymer microshells This type of LbL microshells is composed entirely by pH sensitive block-copolymer has potential application for the encapsulation and triggered release of drugs Li, Hu, et al fabricated via a layer-by-layer technique, templated on $CaCO_3$ particles with built-in polymeric micelles based on polystyrene-b-poly(acrylic acid) [140] This type of LbL microshell can selectively entrap positively charged substances such as rhodamine B and lysozymecan The positively charged substances can be entrapped in the shells where the concentration is much higher than that in the incubation solution The encapsulated compounds shown sustain released to a certain degree, as suggested by *in vitro* release experiments Caruso et al reported using micelles for LbL assembly They synthesis DNA-grafted poly(N-isopropylacrylamide) (PNIPAM) micelles, then assembly PNIPAM micelles into LbL films, and then use poly(ethylene glycol) (PEG) to functionalize the DNA–PNIPAM microcapsules [141] The combination of hydrophobic core and alkyne "click" groups, along with the biodegradability of DNA, offers a multifunctional and versatile DNA–polymer capsule system that can be used for the controlled delivery of therapeutics

Fukui and Fujimoto combined the liposome preparation and the LbL deposition together to prepare hollow shell structures [142] Chitosan was deposited onto a negatively charged liposome surface and form a cationic polymeric layer Then dextran sulfate or deoxyribonucleic acid was used to form an anionic polymers layer They reported that chemical substances with different charges, alendronate, pyranine, and glucose, were encapsulated into microshells where the release rate was suppressed by

the polymer shell wall irrespective of charges [142] Also they use DNA denaturation as a temperature dependent switch to achieve the temperature-dependent release Tabrizian et al developed a delivery system for bone growth factors consisting of a liposome core incorporated into a shell of LbL-assembled natural polyelectrolytes [143] The prepared hydrophilic, monodisperse, spherical and stable cationic nanoparticles (< or =350 nm), as a delivery system, localized the effect of the released bone growth factors within the site of injection in muscle Ramaye et al developed a combination of magnetic liposomes and LbL assembling techniques [144] Superparamagnetic nanoparticles were encapsulated in liposomes prior to the stepwise adsorption of LbL assembly Magnetic field also allows a fast separation of coated liposomes from unbound polyelectrolytes The presence of magnetic nanoparticles and the polyelectrolyte shell opens allows to use external magnetic field to manipulate and target drug carriers

Integrated shell structures have also been proposed De Smedt et al designed self-exploding gel beads that can release micrometer-sized shells at the time of explosion (Figure 2-6) [145] The larger gel beads were loaded with small LbL microshells When the polyelectrolyte coated gel beads explode under alkaline conditions, through rapid hydrolysis of the carbonate esters connecting the polymerized methacrylate groups with the dextran backbone, the smaller LbL microshells become suddenly released Self-exploding gel beads releasing antigen containing LbL microshells at different times after injection could become promising materials for vaccination purposes The reverse-phase was used to coat polymer layers onto agarose microbeads containing tris-buffer for the formation of LbL shell-walls onto the microbeads The polymer-coated agarose microbeads were transferred from an organic to an aqueous solvent where the tris-molecules induced an osmotic pressure in the

microshells' interior The inflation of the LbL microshells caused the expansion of the LbL shell-walls The inflated microshells can control localized chemical or enzymatic reactions that are useful in biomedical applications Ke, et al developed a bi-mode ultrasound/fluorescent imaging agent through LbL assembly of poly(allylamine hydrochloride) (PAH) and CdTe quantum dots onto microbubbles produced by sonication of a mixture of Span 60 and Tween 80 [147] The Quantum-dot-modified microbubbles not only maintained the ability of ultrasound imaging, but also could used as a targeted-drug controlled-release system to deliver the quantum dots by ultrasound targeted microbubble destruction
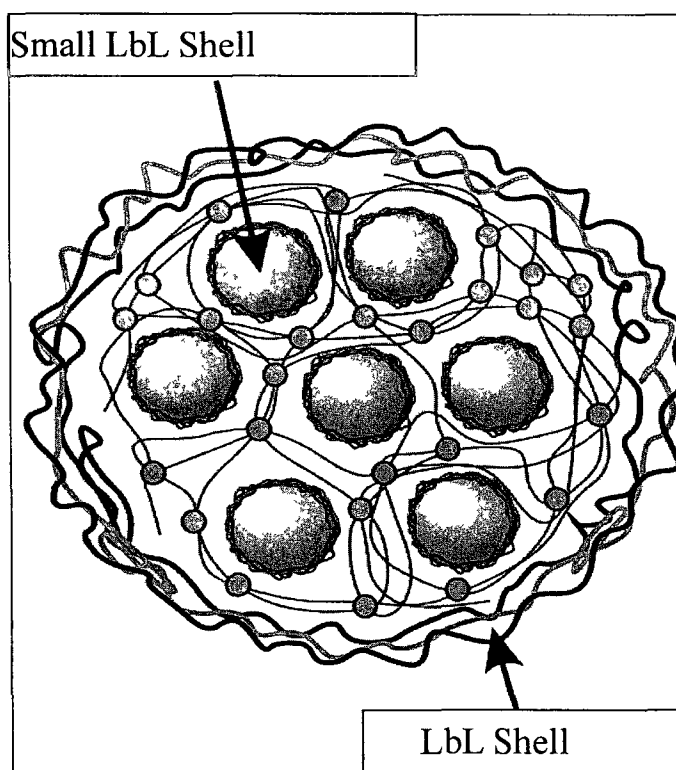
Figure 2-6 Self-exploding polyelectrolyte coated gel beads
releasing micrometer-sized shells at the time of
explosion

In conclusion for Chapter 2, layer-by-layer (LbL) nanoassembly is a simple method allowing the design of multilayer architectures with nanometer precisions It is based on the alternate re-saturated adsorption of oppositely charged components, such as synthetic and natural polyelectrolytes, proteins and nanoparticles The only rule of thumb is sequential adsorption of positively and negatively charged components resulting in any pre-determined composition multilayer film One forms films consisting of bilayers of electrostatically bound cationic and anionic macromolecules, and the typical bilayer thickness is one to a few nanometers Following the first LbL papers published in the beginning of the nineties by G Decher, H Mohwald, Y Lvov, M Rubner and others, one can find around 8,000 publications dealing with the LbL technique It is interesting that until the last few years, the majority of these works were devoted to LbL assembly predominantly using sodium poly(styrene sulfonate) - PSS, poly(allylamine) hydrochloride-PAH and poly(ethyleneimine)-PEI These PSS, PAH, and PEI multilayers are the most studied, but, in recent years, researchers began using natural polyelectrolytes and proteins Now, one can conclude that the LbL method works perfectly for the assembly of anionic compounds, such as alginic acid, hyaluronic acid, chondroitin sulfate, heparin, dextran sulfate, carboxymethyl cellulose, polyaminoacids, DNA, and cationic ones chitosan, dextran amine, polylysine, collagens, protamine sulfate, gelatin A, and others Therefore, we have a group of biocompatible and biodegradable materials (in many cases FDA approved) and the LbL-technique to assemble them in a controllable manner in multilayers of 2-500 nm thickness

How can these architectural multilayers be used for drug delivery? An answer is by formation of microcapsules loaded with drugs Formation of LbL multilayers on tiny

templates and performing LbL encapsulation was first introduced in 1999 in Max Planck Institute, Germany by G Sukhorukov, E Donath, F Caruso, H Mohwald and Y Lvov Generally, LbL encapsulation is the same method as described above for a planar substrate but applied to small 2-5 micrometer diameter drug particles or sacrificed polymeric, $MgCO_3$, $CaCO_3$ or silica cores The possibility to design any thickness or composition of such LbL shells allowed control of drug diffusion from the capsules For different drugs, the variation of the capsule wall thickness within 20-100 nm allowed release time from 10 min to 5 hours This is the main idea for LbL encapsulation for controlled drug delivery

Currently, one can indicate two methods in LbL encapsulation 1) The more common approach for formation of LbL microcapsules on sacrificed cores, dissolution of such cores and loading empty LbL microshells with drugs or proteins through a pH dependable capsule wall pore opening In this case, drug loading is 5-10 % The following drugs were analyzed for LbL encapsulation ibuprofen, furosemide, nifedipine, naproxen, biotin, vitamin K3, insulin, dexamethasone, tamoxifen, paclitaxel 2) The second direction is much less known (only four publications exist from LaTech's group) using the LbL nanoencapsulation of low soluble drug nanoparticles (which allowed ca 70-80 % drug loading)

Therefore, in LbL capsules one can see two tendencies Making microcapsules with sophisticated multifunctional shells of containing 5-10 wt % of drugs and having the ability for switchable release with few to tens of hours In most of the recent published papers, such LbL capsules have a diameter of a few micrometers It appears to be too large for blood injection but these LbL microcapsules have a very thin flexible wall and they have a certain ability to squeeze through narrow capillaries similar to

blood cells   Another tendency is making very thin LbL-shells (two-three polyelectrolyte layers of 5-10 nm) on 100-200 nm diameter cores of low soluble drugs (often anti-cancer drugs)   In this encapsulation, LbL coating provides a strong surface charge producing stable nanocolloids of initially poorly soluble materials   It is this second approach for low solubility cancer drug nanoformulations that will be further developed in this dissertation

CHAPTER 3

INSTRUMENTATION AND MATERIALS

LbL assembly was carried out using polyallylamine hydrochloride (PAH), polyethyleneimine (PEI), protamine sulfate and chitosan, as positively charged polyelectrolytes and bovine serum albumin (BSA), alginic acid, and sodium polystyrene sulphonate (PSS), as negatively charged polyelectrolytes (used at concentration of 2 mg/mL) All polyelectrolytes and albumin were purchased from Sigma-Aldrich except paclitaxel is purchased from LC Laboratories Inc (Woburn, MA), curcumin is provided by Sabinsa Corporation (East Windsor NJ) Deionized water and phosphate buffered saline (PBS) buffer were used at pH 7 2 Ultrasonicator UIP1000hd (Heilscher, Germany) with titanium sonotron was used at a power of 15 W/cm^2 During the experiments, the temperature was controlled at 25-30 °C

Surface potential (zeta potential) and particle size measurements (by light scattering) were performed using ZetaPlus microelectrophoresis (Brookhaven Instruments, Co) Additionally, we used Precision detectors PDExpert light scattering Workstation to check the radius of gyration of our drug nanoparticles A field emission scanning electron microscope (Hitachi S 4800) was used for particle imaging XRD experiments were performed with the help of a Bruker D8 Discover X-ray Diffracto-meter to determine the crystalline structure of drug nanoparticles

28

The drug release rates of nanocapsules with different shell composition were measured using standard 1 mL horizontal diffusion chambers with 0 2 μm cellulose acetate membranes The drug dispersion was placed to the side of the diffusion chamber containing a magnetic stirrer and the drug was released against the same volume of PBS, pH 7 2 to mimic the sink conditions expected *in vivo* The concentration of released drugs in PBS was dissolved in ethanol at 1 1 (v/v), centrifuged to remove insoluble polyelectrolytes and measured with a UV spectrophotometer (Agilent 8453 Wavelength range 190-1100 nm) Curcumin was measured at 490 nm, and paclitaxel was measured at 245 nm Also the same measurements were done to calculate product yield at the end of sonication Further, we describe the instruments used in this work in more detail

3 1 Ultrasonicator

A Hielscher UIP1000hd ultrasonic processor, Figure 3-1, was used to prepare nanoparticles in this research
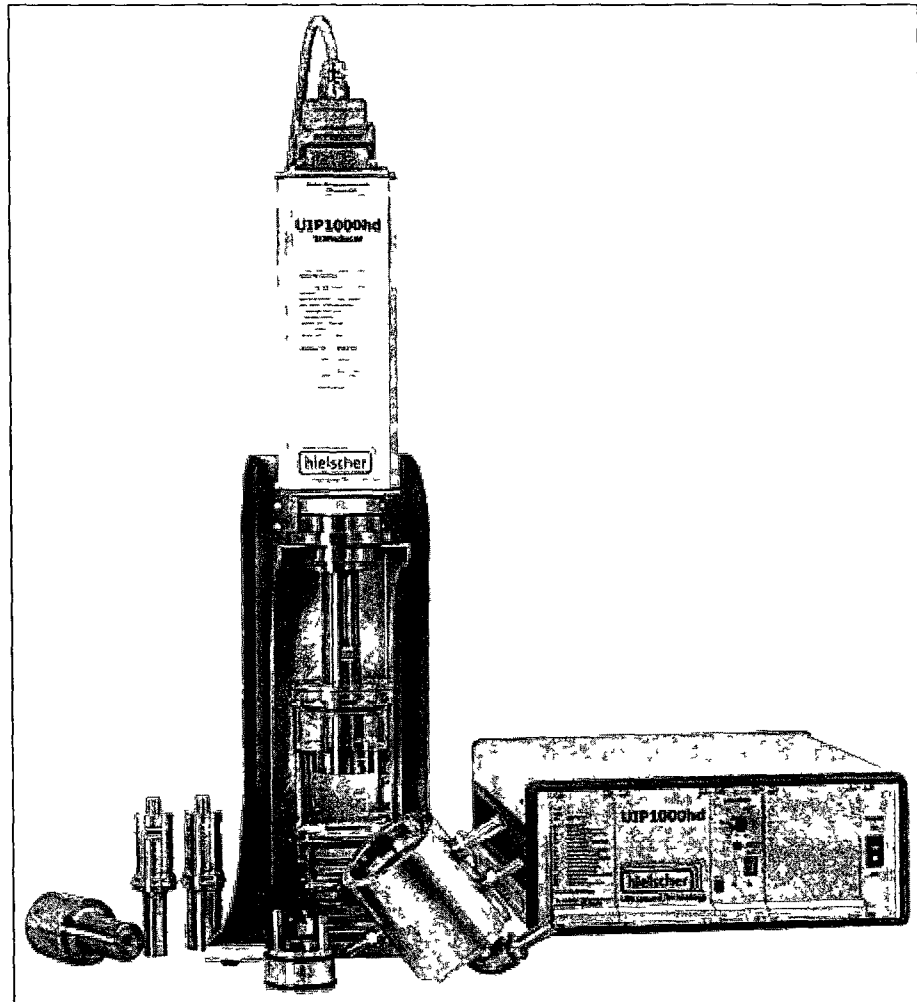
Figure 3-1 Hielscher UIP1000hd ultrasonic processor

When ultrasonic energy is applied to liquids, and if amplitude and acceleration are high enough, the phenomenon of cavitation occurs The cross-section of sonotrin used corresponded to the surface area of the drug dispersion to maximize ultrasonication power The liquid bursts and vacuum bubbles are generated during the alternating high-pressure and low-pressure cycles When these small bubbles cannot absorb more energy, they implode during a high-pressure cycle, so pressures up to 1,000 bar and shock waves as well as liquid jets of up to 400 km/h are reached locally These intense forces, caused by ultrasonic cavitation, take effect on the enclosing

droplets and particles The main objective of power ultrasonics consists of cavitational forces, with heating being mostly a welcome side-effect Cavitation and the effects described above cause interparticle collision

3.2 Zeta Potential Analyzer

A ZetaPlus zeta potential analyzer (Brookhaven Instruments, Co), Figure 3-2, was used to measure the surface charge of nanoparticles during the LbL assembly process This instrument also can be used to measure the particles hydrodynamic diameter using light scattering
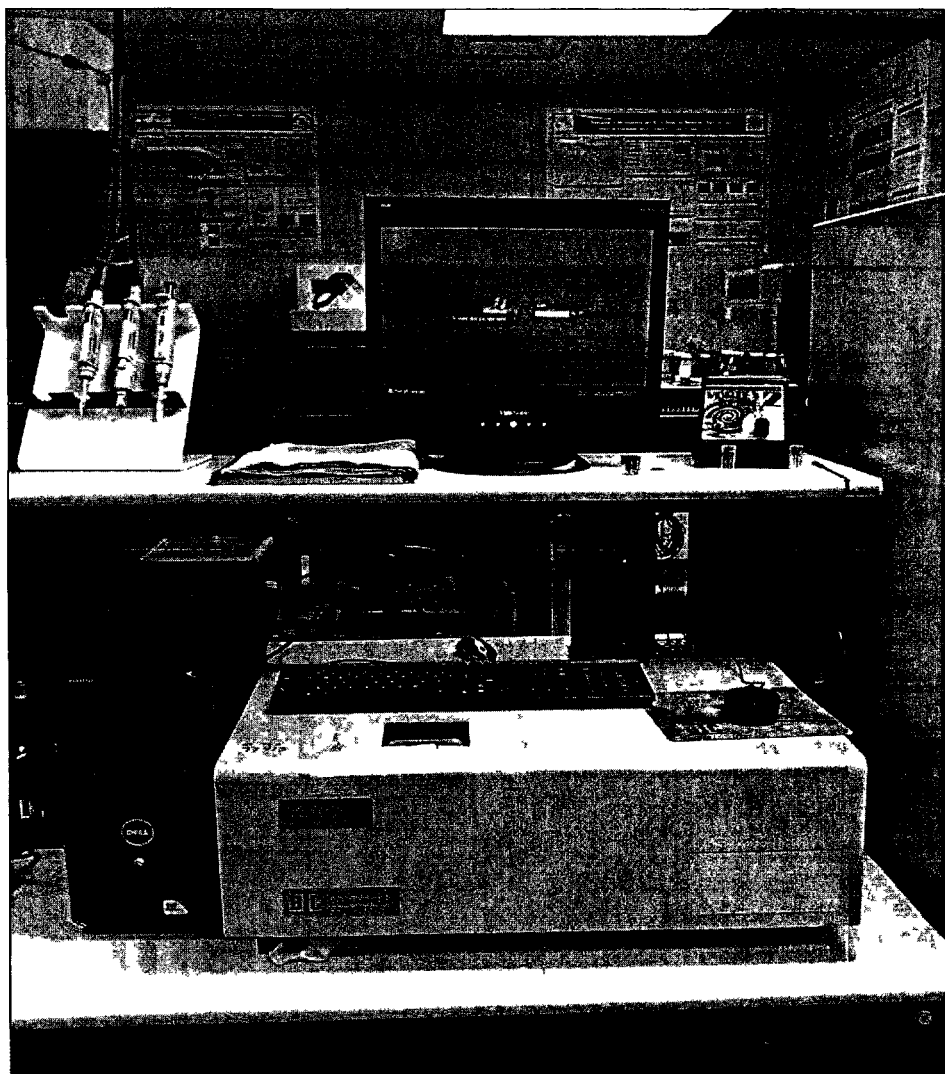
Figure 3-2 Zeta potential analyzer by Brookhaven Instruments, Co.

Zeta potential meassurement was calibrated using a BI-ZR3 zeta potential reference material provided by Brookhaven Instruments, Co.

100 mg of BI-ZR3 was added to 20 mL of the 1 mM KCl, result in 5mg/mL concentrate. Then the concentrate dilutes to 1.25×10^2 mg/mL. This standard sample is used to have a mean zeta potential value of 53 mv ± 4 mv, and 300 nm mean size.

Zeta potential is used as a surrogate for surface change and is often measured by observing the oscillations in signals that result from light scattered by particles located

in an electric field, though there are other approaches There are a number of instrumental configurations by which this is achieved, mostly using a doppler shift, and the users should familiarize themselves with the particular approach implemented in their equipment Instrumentation concerns aside, the need for dilution begs the question of what is an appropriate diluents, because its choice can profoundly influence the surface chemistry and thus the results This analyzer was calibrated using a BI-ZR3 reference material from Brookhaven Instruments, Co

3.3 Dynamic Light Scattering

The Precision detectors PDExpert light scattering workstation Figure 3-3 is a multi-detector light scattering platform that can be employed for light scattering measurements on a static sample (e g a test tube) or for flow through measurements (e g high performance liquid chromatography, gel permeation chromatography and size exclusion chromatography) The workstation is designed to provide the ultimate in detection for characterization of polymers, nanoparticles, lipids, colloids and proteins
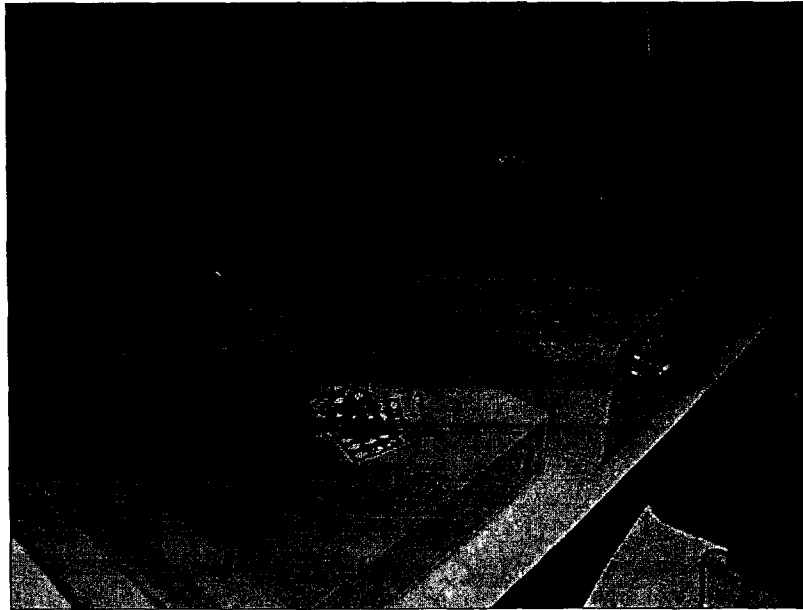
Figure 3-3 Precision detectors PDExpert light acattering
workstation

DLS, also known as photon correlation spectroscopy (PCS) or quasi-elastic light

scattering (QELS) records the variation in the intensity of scattered light on the

microsecond time scale. This variation results from interference of light scattered by

individual particles under the influence of Brownian motion, and is quantified by

compilation of an autocorrelation function. This function is fit to an exponential, or

some combination or modification thereof, with the corresponding decay constants

being related to the diffusion coefficients. Using standard assumptions of spherical size,

low concentration, and known viscosity of the suspending medium, particle size is

calculated from this coefficient. The advantages of the method are the speed of analysis,

lack of required calibration, and sensitivity to submicrometer particles. Drawbacks

include the necessity of significant dilution to avoid artifacts, the need for cleanliness in

sample preparation, the mathematical instability of the procedure used to extract decay

constants, and the possible influence of interparticle interactions. DLS is a stand-by

method for those working in the area of nanoparticles because of the simple measure requirement

3.4 X-Ray Diffractometer

A Bruker D8 X-Ray diffractometer was used to determine the crystal structure of the nanoparticles (Figure 3-4)
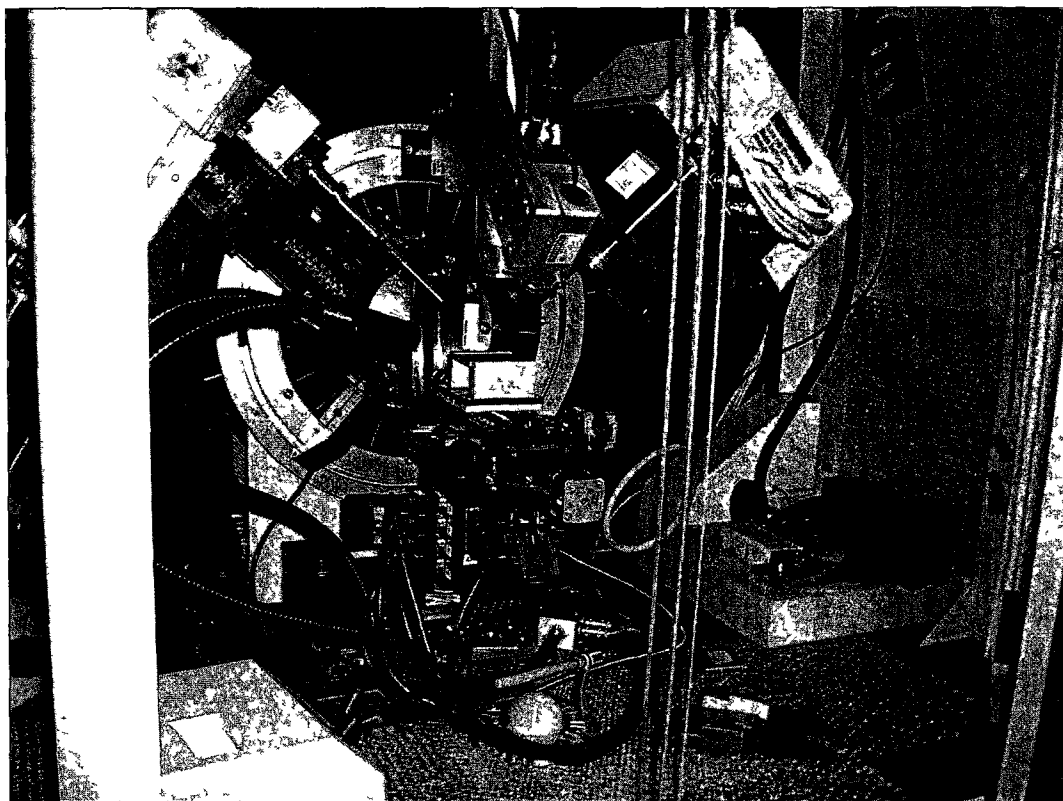
Figure 3-4 Bruker D8 Discover X-ray diffractometer

3.5 SEM

Figure 3-5 shows the Hitachi SEM which was used for nanoparticles visualization Diluted drug nanoparticles dispersion was dropped on a suitable substrate and coated with a ca 0 5 nm gold layer to provide conductivity
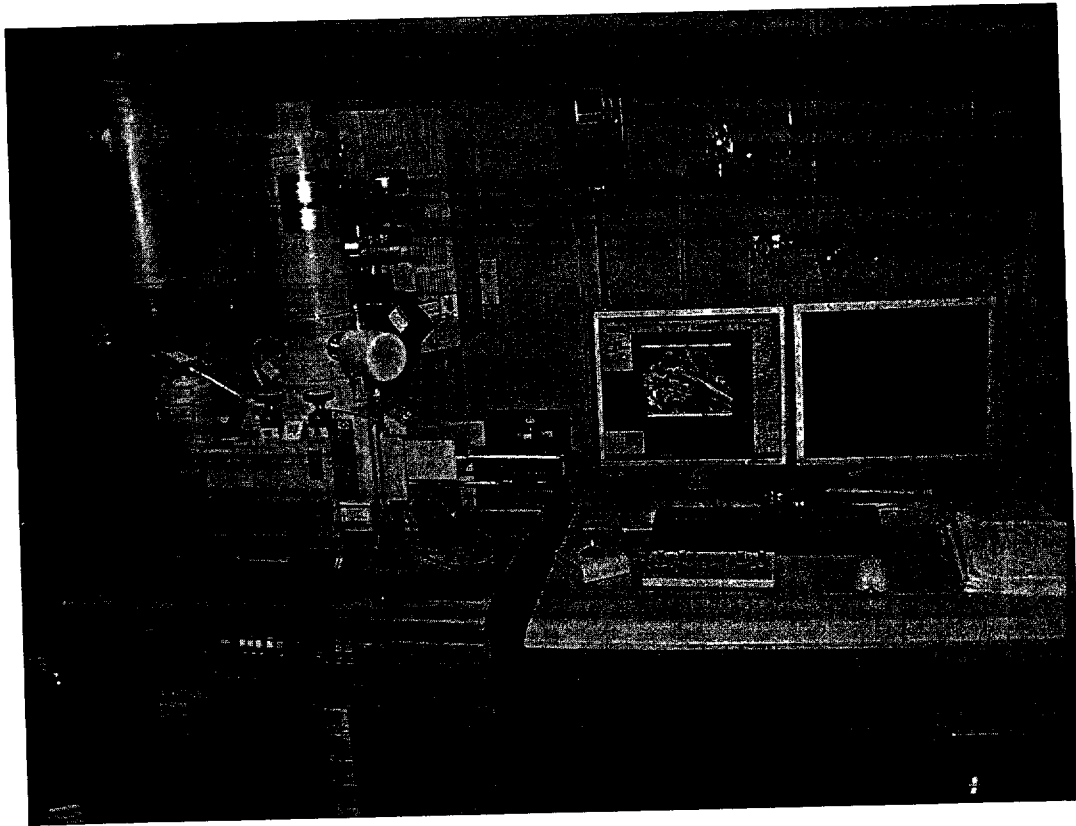
Figure 3-5 Hitachi S-4800 scanning electro microscope

This SEM also has an energy-dispersive X-ray spectroscopy (EDX) detector (EDAX Sapphire). EDX Analysis can be used to determine the element composition of the sample.

3.6 Ultra Violet Spectrophotometer

An UV-vis spectrophotometer (Agilent 8453), Figure 3-6, was used to measure the concentration of drug in the release test. The drug release test measures the pharmacodynamic diffusion of the nano drug particle in a side-by-side diffusion chamber.
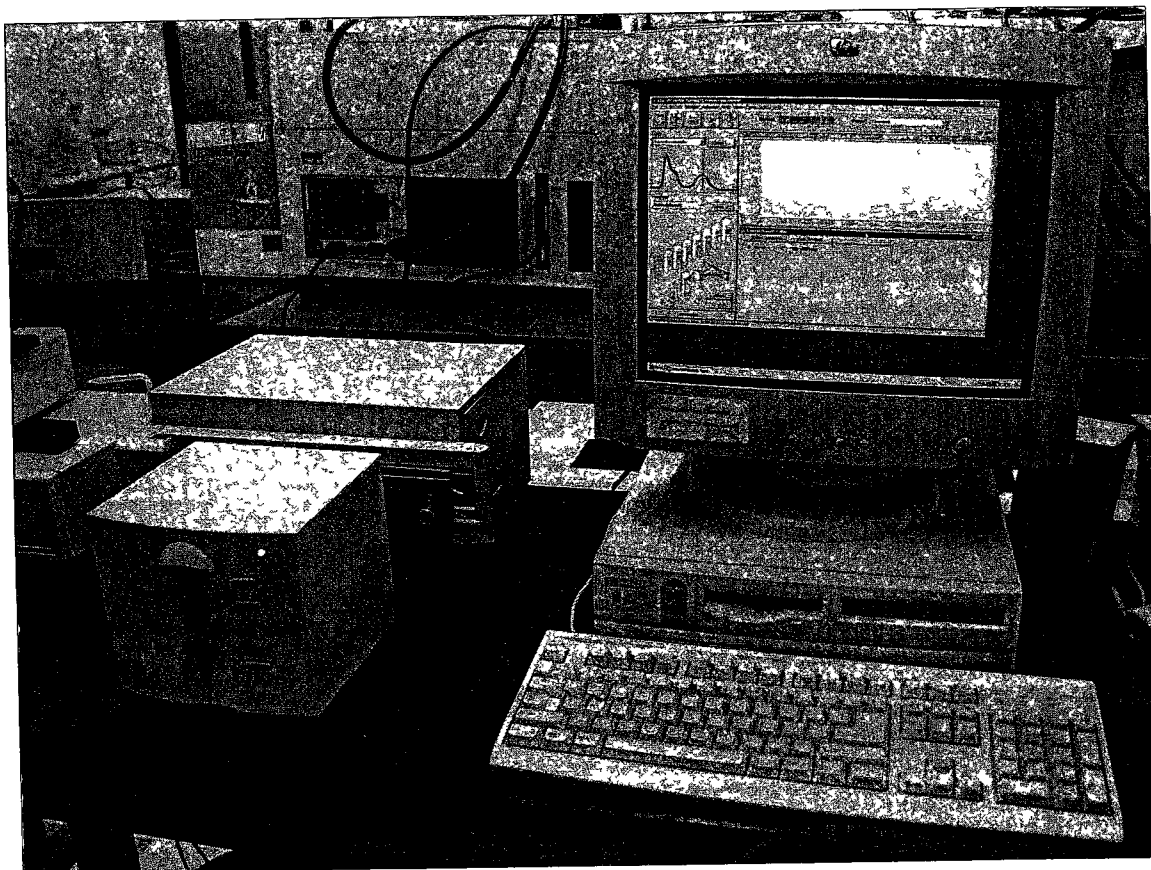
Figure 3-6 Agilent 8453 UV-Vis spectrophotometer

CHAPTER 4

DRUG NANOPARTICULATION VIA TOP-DOWN APPROACH

Nanoparticle drug carriers were developed using a combination of ultrasonication and encapsulation with synthetic and biodegradable polyelectrolytes Two different approaches to attain the desired featured properties are the "top-down" and "bottom-up" synthetic methods These two methods are described in Chapters 4 and 5 A common feature of these two related methods is ultrasonication-driven formation of drug nanocores accompanied by a simultaneous polycation coating providing aqueous colloidal stability The "top-down" method was more efficient in the preparation of large amounts of 200-250 nm diameter paclitaxel capsules, and the "bottom-up" approach allowed for the formation of smaller capsules of ca 100 nm diameter but with less product yield Some sections of these two chapters were published in papers written by the author of this dissertation and will be correspondingly referred [148] and [149]

4.1 Methodology

Powerful ultrasound generates micro-bubbles in a liquid These micro-bubbles collapse in microseconds If any solid particle is near the bubble during the collapsing, jets of fluid and shock waves will hit the particle and break it up While adding polyelectrolyte into the solution, the typically negative surface of the newly formed

38

drug surface will help to keep particles from aggregation Thus, a smaller particle size can be achieved with a better size distribution Because the ultrasonication process breaks down the particles, it is a mechanical process The formed particles will have a wide range of sizes Both power and sonication time effect the nanoparticles' size distribution In general, the higher the power and the longer the time, the smaller the particles will be But if one stops sonication, particles will aggregate To prevent the aggregation during the sonication and increase the efficiency of the sonication, we added polycations that adsorbs onto the drug nanoparticles and prevents re-aggregation The minimum amount of polycation needed for complete coverage was calculated in Appendix A The surface zeta potential of the particles changed to positive during the polycation adsorption and reached of ca + 40mV

For drug encapsulation, anionic sodium polystyrene sulfonate (PSS) of MW 70 KDa and cationic poly(dimethyldiallyl ammonium chloride) (PDDA) of MW 100 KDa were sequentially adsorbed onto the particles of different drugs at pH 6, and then the desired number of layers in the capsule shell was fabricated Biodegradable polyelectrolytes that were used for the LbL assembly are protamine sulfate and chondroitin sulfate The multilayer shells that are fabricated on the drug help in prolonging the release of the drug Figure 4-1 shows the scheme for top-down approach The verification of the alternation of surface charges and particle size were done with a ZetaPLus Brookheaven microelectrophoretic zeta-potentiometer A visualization of the fabricated microcapsules was completed using SEM
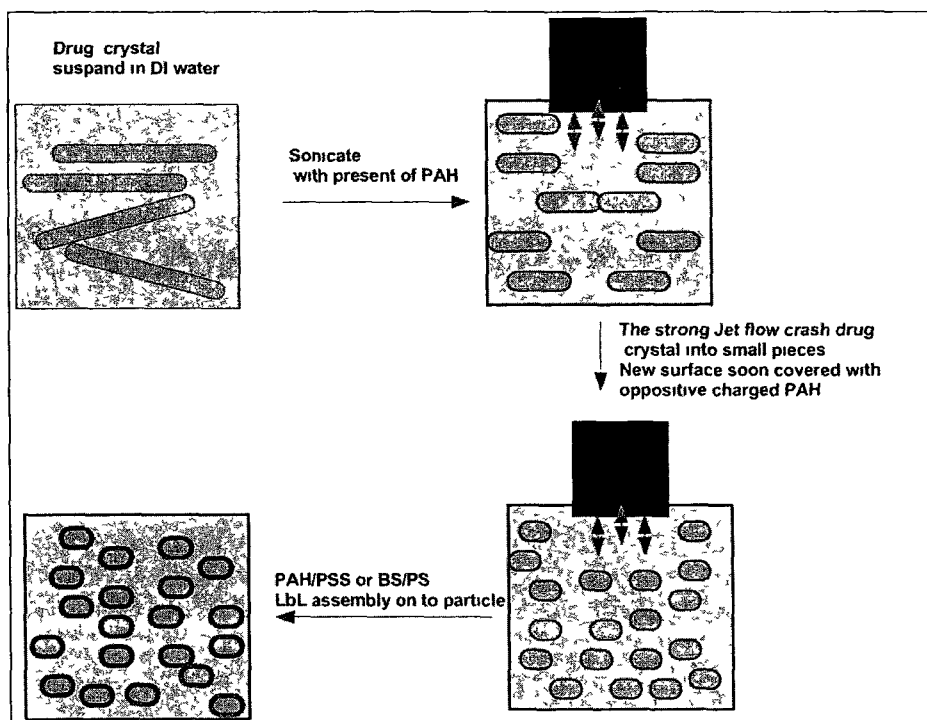
Figure 4-1 Scheme for top-down approach

4.2 Curcumin Nanoformulation

Curcumin is a well known natural compound traditionally used as a food additive or a health nutrient supplement in many oriental countries Recently, its anticancer activity was recognized [150] It is a low soluble compound (the aqueous solubility is ca 0 01 mg/mL) The curcumin structural formula is shown in Figure 4-2
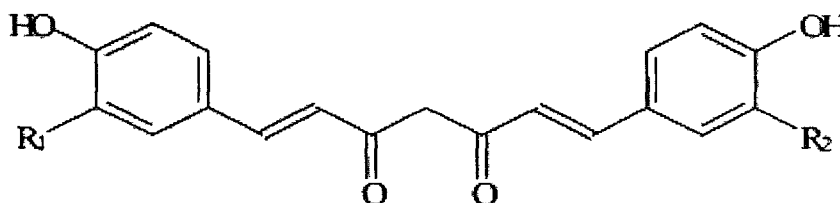
Figure 4-2 Structural formula for curcumin

4.2.1 Preparation of curcumin nanoparticles

The following experimental step-by-step sequence was used to prepare nanoparticles of curcumin

1) 10 mg curcumin powder was mixed with 10 ml of DI water

2) The mixture was pre-sonicated for 5 min to form curcumin suspension

3) 2 mL of 1 5 mg/mL cationic PAH were added to the suspension

4) 45 min sonication was applied

5) The curcumin nanoparticles were washed twice with DI water using centrifugation at 7000 rpm (5204 g rcf) for 10 min to separated nanoparticles from supernatant and re-dispersed in 20 mL of DI water

6) 2 mL of 3 mg/mL anionic PSS were added to the mixture, 10 min of reaction time was allowed for the polyelectrolyte adsorption

7) The supernatant was removed by centrifugation at 7000 rpm Nanoparticles were washed with DI water and re-dispersed

8) Steps 6-7 were repeated for next layer of cationic PAH

9) Steps 6-8 were repeated several times to achieve the desired number of polyelectrolyte layers in the coating

Instead of cationic PAH and anionic PSS, biodegradable polyelectrolytes such as protamine sulfate (PS), bovine serum albumin (BSA) and chondroitin sulfate (ChS), may be used for the coating

The alternation of electrophoretic (ξ) potential demonstrates a step-wise formation of the LbL-shell consisting of cationic PAH and anionic PSS on curcumin nanoparticles Figure 4-3 shows a typical zeta potential change during the ultrsonic assisted LbL assembly process Each sample was measured 10 times The standard

deviation was given by the zeta potential analyzer After the initial -50 ± 2 mV for bare curcumin particles, PAH adsorption during the first step of nanoparticles synthesis converts the potential to +30 ± 2 mV Next, anionic PSS adsorption changes the potential to -53 ± 2 mV, followed by +20 ± 2 mV with PAH, and again -50 ± 2 mV with PSS Therefore, a multilayer coating of polycations and polyanions with composition of (PAH/PSS)$_2$ was coated onto the curcumin nanoparticles and the enhanced surface potential of -50 mV was reached This value is well above commonly accepted colloidal stability threshold of (±) 30 mV [149]
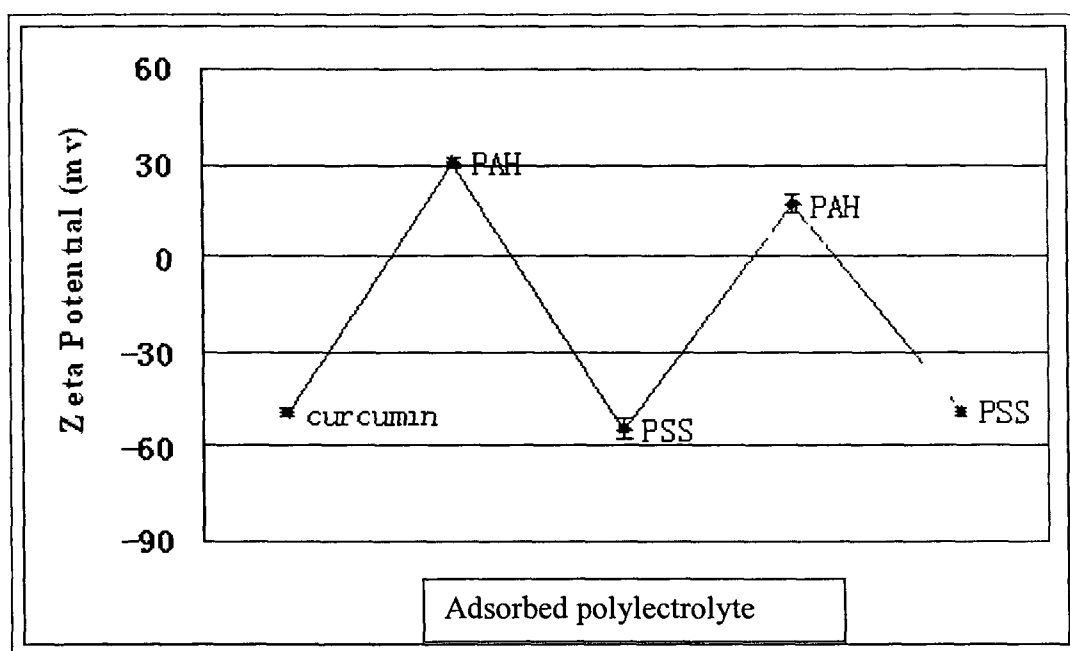
Figure 4-3 ξ-potential alternation during LbL-shell formation of cationic PAH and anionic PSS on curcumin nanoparticles Standard deviation shows the same sample run 10 times on zeta potential analyzer

Separate QCM analysis of the LbL assembly process for these polyelectrolytes on silver plated 9-MHz Quartz Crystal Microbalance resonators (USI-System Instr, Japan) demonstrated a thickness increment of 2 0 ± 0 3 nm for a PAH/PSS bilayer, and

the total thickness of the two-bilayer shell on the curcumin nanoparticles may be estimated as ca. 4 nm. Any shell composition may be achieved with further alternate adsorption of polycations and polyanions [149].

In another experiment, curcumin nanocapsules with two bilayer shells of biocompatible protein materials were produced. A positive layer in the shell was generated using protamine sulfate (PS), while bovine serum albumin (BSA) formed a negative layer. Total composition produced was (PS/BSA)$_2$. For these LbL nanocapsules, zeta potential also regularly alternates between +30 mV and -50 mV providing high colloidal stability of the samples [149]. The dispersion of the nanoparticles with the concentration of 0.2 g/mL was stored in DI water for two weeks without precipitation.

The yield of the nanoparticles was about 30-40 % which means that, if curcumin concentration at the beginning of the process was typically 1 mg/mL, then, in the product, it was of about 0.3-0.4 mg/mL.

Figure 4-4 shows SEM image of the formed curcumin nanoparticles. One can see that, in diluted dispersions, the nanoparticles' size is from 50-120 nm (left) and, upon the drying of the concentrated sample, some aggregation occurs (right image).
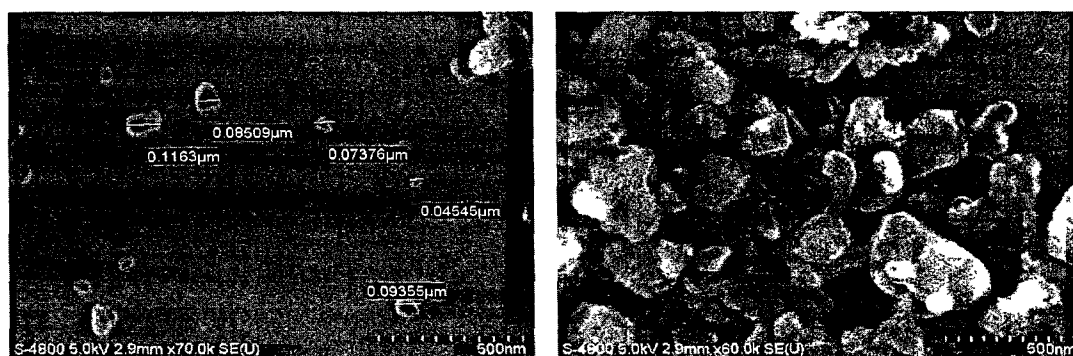
Figure 4-4 SEM image of the formed curcumin nanoparticles (left) diluted sample, and (right) concentrated sample

4.3 Nanoformulation of Paclitaxel

Paclitaxel (Figure 4-5) is an efficient anti-cancer drug, but due to very low solubility, there is not effective way for its delivery However, with paclitaxel nanoformulation it is feasible to increase the drug concentration a hundred times (up to a few mg/mL)
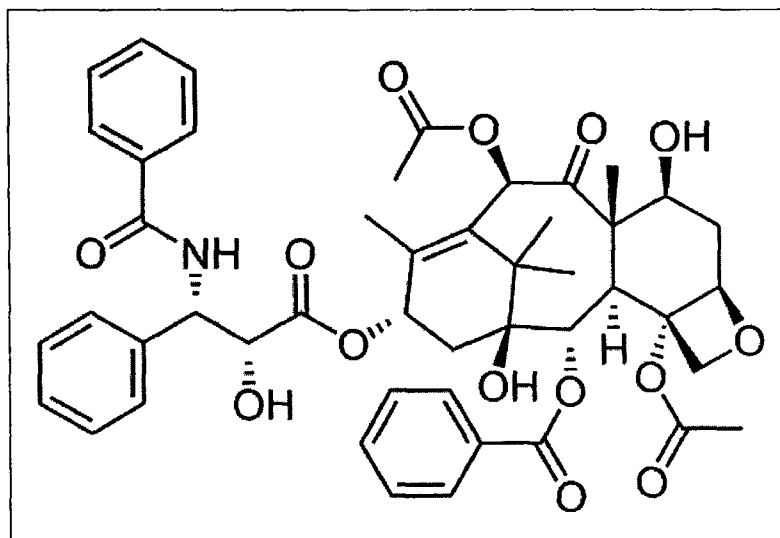
Figure 4-5 Structural formula for paclitaxel

Figure 4-6 shows a typical zeta potential change during the assembly Each sample was measured 10 times The standard deviation was given by the zeta potential analyzer One can see the zeta potential changes for the LbL assembly of polyelectrolyte multilayer shell on paclitaxel nanoparticles Initially, the surface potential of the paclitaxel nanoparticles was -21 mV After deposition of the first cationic PAH layer (with simultaneous ultrasonication) we obtained the particle surface potential of 24 ± 3 mV After deposition of the second layer, anionic polyelectrolyte layer (PSS), we increased the magnitude of zeta potential to 41 ± 3 mV, and finally, at the last deposition step a coating with biodegradable chitosan/alginic acid (blue line) or

albumin (red line) gave us a strong negative surface charge of the encapsulated paclitaxel of - 46 ± 4 mV and -32 ± 3 mV This high surface potential provided for the stability of the developed paclitaxel nanocolloids for at least two weeks at concentrations of 0 5 mg/mL
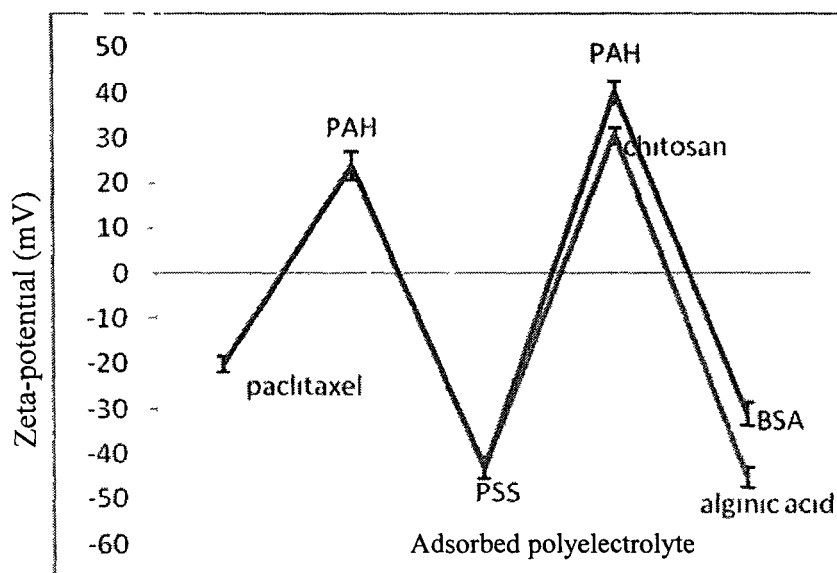
Figure 4-6 ξ-potential of paclitaxel coated with two different
bilayers of PAH-PSS-PAH-BSA and PAH-PSS-
chitosan-alginic acid (using top-down approach)
Standard deviation shows the same sample run 10 times
on zeta potential analyzer

In Figure 4-7, one can see the SEM image of the initial micronized sample of paclitaxel It consists of needle-like rods with diameter of ca 100 nm and length of 2-3 μm During sonication-assisted LbL encapsulation, we obtained rather homogeneous particles with overage sizes of 100 × 100 × 200 nm This particle suspension is collapsed during the drying of the sample but the aqueous dispersion itself is stable It is interesting, that due to very low solubility, it is possible to keep the paclitaxel sample without dissolution for weeks because in such a restricted volume the supernatant

saturation is reached preventing further particles dissolution. Only in a big solvent volume (under sink release conditions), can paclitaxel nanoparticles be partially or completely dissolved. These particles are less than 300 nm and are in accordance with the minimum particle size allowed by FDA for medical injections.
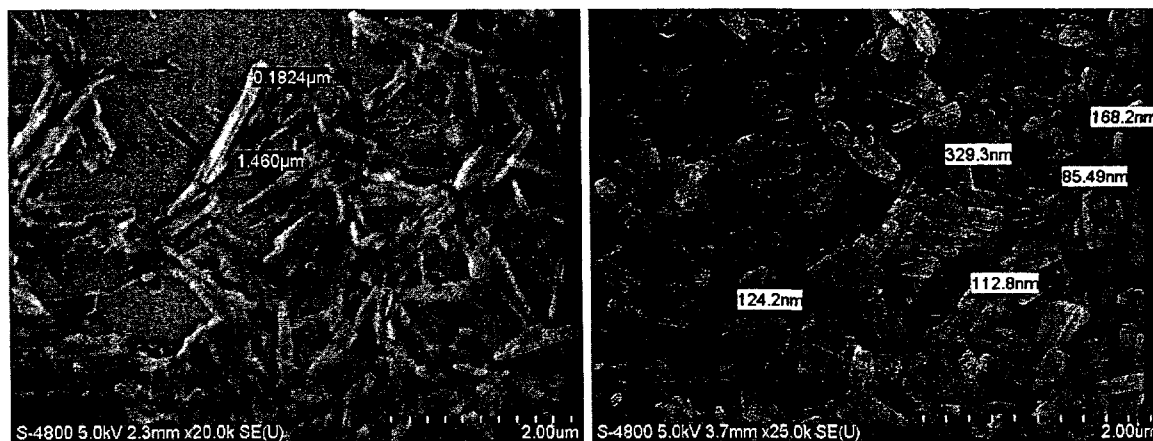
Figure 4-7 SEM image of orginal paclitaxel (left) and after
ultrasound assisted LbL encapsulation with
PAH/PSS/chitosan/alginic acid (right)

CHAPTER 5

DRUG NANOPARTICULATION VIA BOTTOM-UP APPROACH

This technology is our new invention It was disclosed to LaTech 1) Z Zheng, Y Lvov "Sonication synthesis of polyelectrolyte coated nanoparticles through mixing molecular solutions with bad solvents," September 30, 2008-27, and 2) Y Lvov, Z Zheng, V Torchilin "Paclitaxel and atavoquone nanoparticle production through ultrasonication with gradual desolvation assisted with polycation coating Synthesis of the mixed drugs nanoparticles," December 1, 2008-30 US patent application by V Torchilin, Y Lvov, Z Zheng "Stable Aqueous Nanocolloids of Paclitaxel and Atavoquone," was filed by Louisiana Tech University and Northeastern University on April 25, 2009 Some sections of this chapter were published in a paper written by the author of this dissertation and will be correspondingly referred [149] Z Zheng, X Zhang, D Carbo, C Clark, C-A Nathan, Y Lvov, Langmuir, v 26, 7679-7681, 2010 "Sonication assisted synthesis of polyelectrolyte coated curcumin nanoparticles "

5.1 Methodology

The drug powder was dissolved in ethanol/water solution After drug has been completely dissolved, we added aqueous polycations, poly(allylamine hydrochloride) (PAH) or biodegradable protomine sulfate (PS), and started ultrasonication with a UIP1000, Hielscher instrument, at energy density of 100 Wt per mL of solution During

the sonication, water was slowly added into the solution Because of the added water, the solvent becomes more polar, causing a decrease of drug solubility, and eventually, its concentration exceeds the solubility threshold resulting in the drug supersaturated conditions Then, crystal nucleation starts Under high power ultrasonication, the drug particle growth ceases at the initial stages [149] An adsorption of polyelectrolytes onto the drug nanocrystals establishes a barrier for their further growth and aggregation The minimum amount of polyelectrolytes needed for complete coverage was calculated in Appendix A Obtained drug crystal particles were stable and did not aggregated after sonication was stopped We assume that it was because of the increase of surface charge provided by the adsorbed polyelectrolyte layer After 45 min of sonication, drug nanocrystals were separated from the solution by centrifugation and re-suspended in DI water Additional polyelectrolyte multilayers were built on the curcumin nanoparticles by alternate adsorption of polyanions and polycations (LbL shell assembly) For biocompatible capsules, an alternate adsorption of cationic protamine sulfate (PS) and anionic bovine serum albumin (BSA) were used (Figure 5-1)
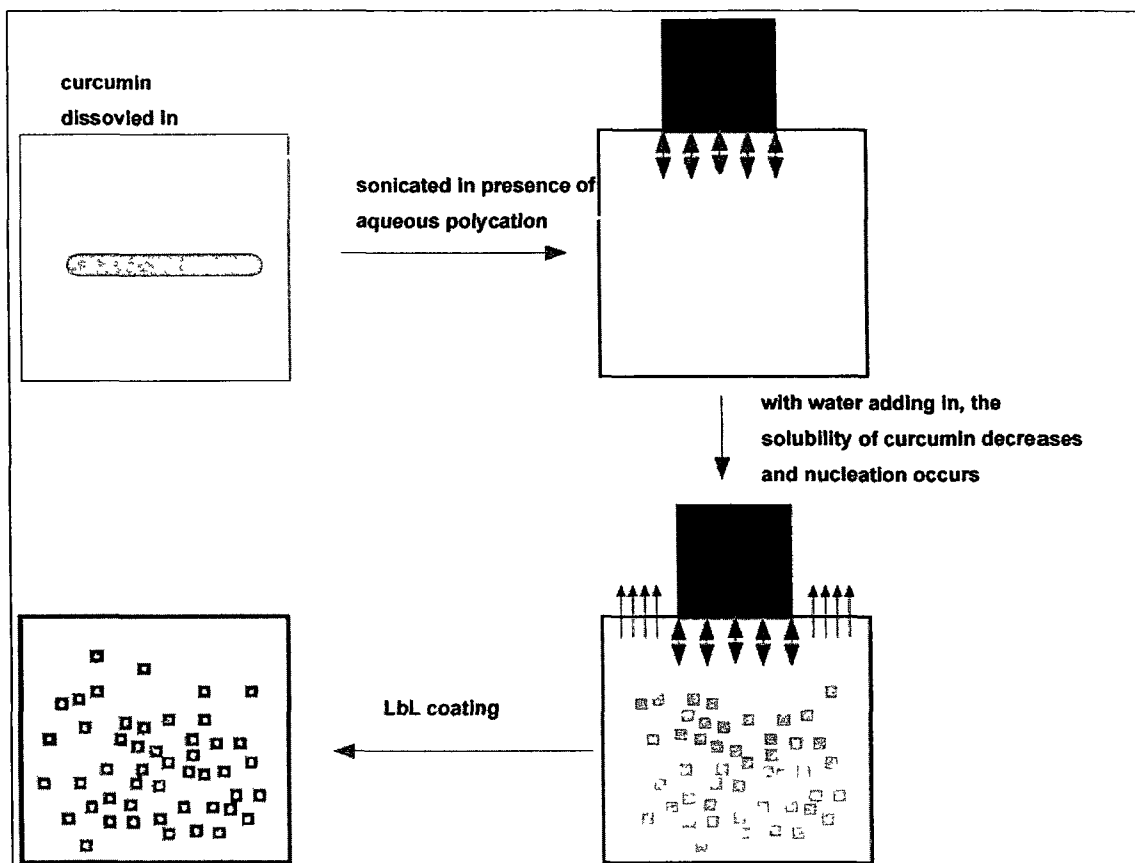
Figure 5-1 Scheme of the bottom-up curcumin LbL
nanoformulation

The drug was dissolved in 60 % ethanol at a concentration of 2 mg/mL We present here the results for low solubility anti-cancer drugs curcumin and paclitaxel Ultrasonication was applied for 45 min while slowly adding water at the rate of 0 2 mL/min [149]

5.2 Curcumin Nanoformulation

5.2.1 Nanocurcumin preparation

The drug/shell multilayer structure is curcumin/PS/BSA/PS/BSA

The following experimental step-by-step sequence was used to prepare nanoparticles of curcumin

1) 10 mg curcumin were dissolved in 10 ml of 60 % ethanol/water (optionally, we also used acetone)

2) The solution was presonicated for 5 min to completely dissolve the curcumin

3) 6 mL of 0 2 mg/mL aqueous cationic PS, pH 6 5 were slowly added at a speed of 0 5 mL/min during 30 min sonication This is the key step of the procedure initiating the particle nucleation

4) The nanoparticles were washed twice with DI water using 7000 rpm centrifugation to separate the nanoparticles from supernatant

5) 3 mg of anionic BSA were added to the mixture and allowed to adsorb for 10 min

6) The nanoparticles were washed twice with DI water using 7000 rpm centrifugation before coating with aqueous cationic PS

7) 3 mg of PS were added to the mixture and allowed to adsorb for 10 min

8) Steps 4-7 were repeated to achieve a given number of layers

Figure 5-2 shows a typical zeta potential change during the ultrsonic assisted LbL assembly process Each sample was measured 10 times The standard deviation was given by the zeta potential analyzer Due to the adsorption of cationic PAH, the surface potential of these nanoparticles was positive ca +30 mV Further coating with PSS increased the zeta potential magnitude to -52 ± 4 mV High surface charge increases colloidal stability for this formulation For example, in an aqueous curcumin nanocolloid of 0 5 mg/mL concentration a stable dispersion of the drug was preserved for one month In Appendix B, we calculated the average distance between particles

under different conditions Low concentration means longer distance between particles, which usually means better stability
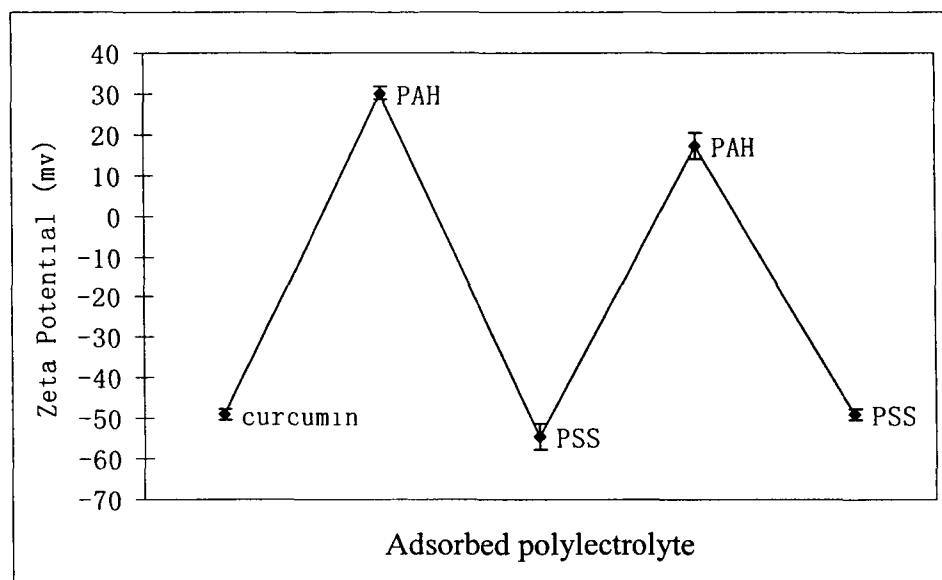
Figure 5-2 Particle ξ-potential alternation during LbL coating of
curcumin (pH 6 5) Standard deviation shows the same
sample run 10 times on zeta potential analyzer

Curcumin nanoparticles of rectangular shape were obtained Edges from 60 nm to 90 nm (Figure 5-3) and average edge size of 80 ± 20 nm were estimated with SEM imaging processing software Quartz PCI (Hitachi) and light scattering experiments (Brookhaven Instruments, Co , ZetaPlus) The rectangular shape of the nanoparticles is associated with the crystalline nature of the obtained curcumin particles [149]

0.05274μm

0.09632μm

0.04680μm

0.05974μm

0.06056μm

S-4800 5.0kV 7.5mm x7.00k SE(U) 8/2/2007 11:20   5.00um   S-4800 5.0kV 3.1mm x40.0k SE(U)   1.00um
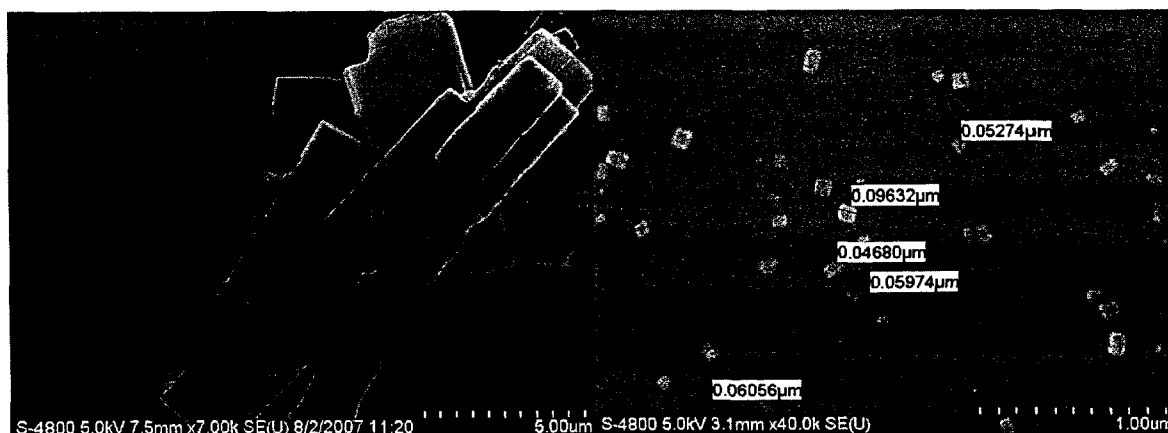
Figure 5-3 SEM images of initial curcumin powder (left) and
resulting curcumin nanocolloid (right)

To examine the crystal structure of the curcumin nanoparticles, X-ray powder

diffraction analysis was carried out with a Bruker-D8 XRD instrument. Bragg peak

positions in the X-ray pattern obtained from the dried nanoparticles powder coincided

with the peak positions for bulk curcumin powder, but the peaks were wider due to

smaller crystallite size (Figure 5-4). These X-ray data indicate that the crystal structure

of curcumin was preserved, and polycations added during drug crystal formation did not

form a complex with curcumin molecules but only covered the crystals surface. We

assume that polycations were layered predominantly on the crystal surface, as it follows

from electrophoretic (ξ-potential) data given below [149].
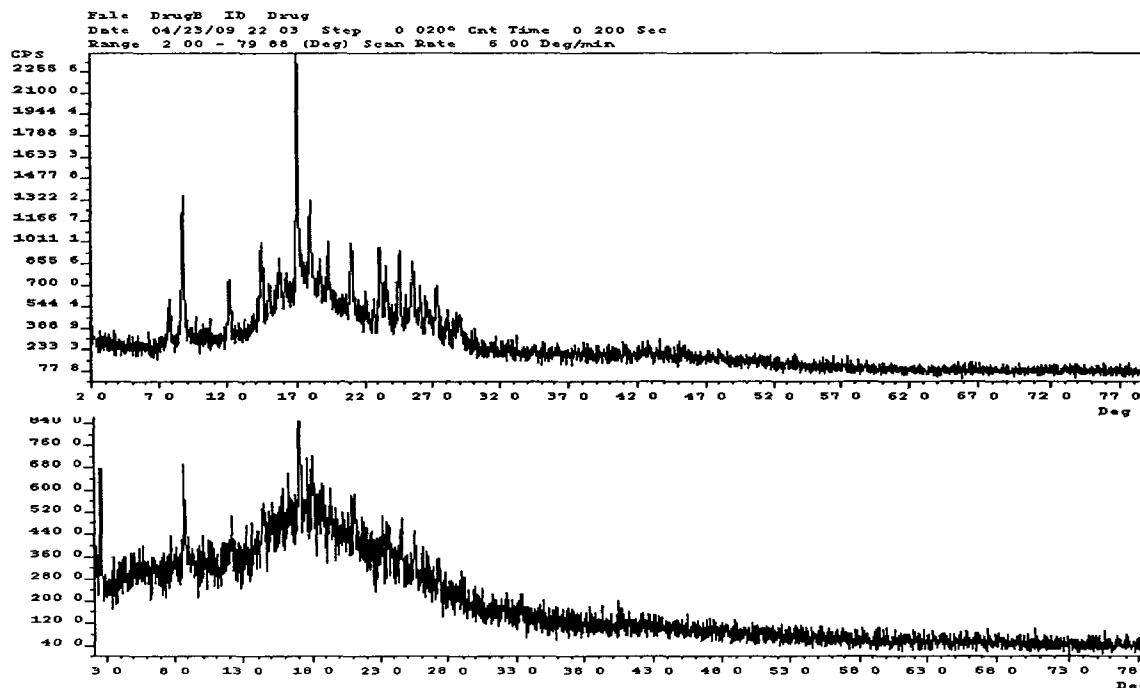
Figure 5-4 X-ray diffraction spectra for micronized curcumin
powder (upper spectrum) and for nanoformulated
curcumin (lower spectrum)

5 3 Paclitaxel Nanoformulation

5.3.1 Preparation of nanopaclitaxel

The following experimental step-by-step sequence was used to prepare

nanoparticles of paclitaxel

1) 10 mg of paclitaxel were dissolved in 10 mL of 60 % ethanol/water

solvent

2) The mixture was presonicated for 5 min to completely dissolve paclitaxel

3) 6 mL of aqueous 0 2 mg/mL cationic PS (pH 6 5) was added at a speed of

0 5 mL/min during 45 min sonication This is the most important stage of

the formulation

4) The nanoparticles were separated from supernatant using 7000 rpm centrifugation for 10 min and washed twice with DI water Then the nanoparticles were redispersed in 10 ml of DI water

5) For next BSA layer, 3 mg BSA were admixed to the dispersion for 10 min

6) Step 4 was repeated

7) A layer of cationic protamine sulfate was deposited in the same way as in step 5

8) Step 4 was repeated

9) Steps 5-8 were repeated to obtain the desired coating structure

Paclitaxel was dissolved in a "good" solvent (60 % ethanol/water or 60 % acetone/water) After dissolution of the drug at high concentration, ultrasonication was started with aqueous polycation slowly added to the solution With an increase of water concentration, solubility of paclitaxel decreased, reached saturation and the nucleation began resulting in the formation of nano-size particles

Powerful sonication prevents formation of larger drug particles and polycation adsorption provides for a surface charge sufficient for colloidal stability After a 45 min treatment, the drug particles were centrifuged at 7,000 rpm for 10 min and re-suspended in distilled water The second layer of anionic polyelectrolytes was deposited to maximize the capsule surface potential Nonreacted polyanions were removed by centrifugation and paclitaxel nanoparticles with the average particle size of 100 nm were obtained Additional polyelectrolyte layers may be further built up on the drug nanoparticles using the traditional LbL process without sonication Obtained paclitaxel nanocolloid was kept in a small volume of saturated solution to prevent drug release [149]

Figure 5-5 shows a typical zeta potential change during the Ultrsonic assisted layer-by-layer assembly process Each sample was measured 10 times The standard deviation was given by the ZetaPlus zeta potential analyzer (Brookhaven Instruments, Co) The alternated zeta potential during formation of LbL nanoshells on paclitaxel nanocores has a minimal potential of -35 mV
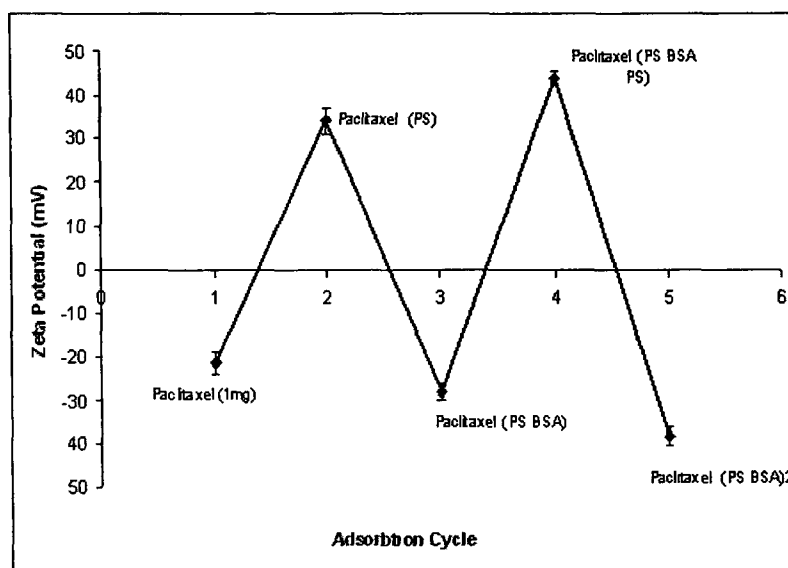
Figure 5-5 ξ-potential change during the LbL encapsulation of
paclitaxel Standard deviation shows the same sample
run 10 times on zeta potential analyzer

Figure 5-6 shows SEM image of the resulting nanocapsules with average diameter of 90 ± 20 nm
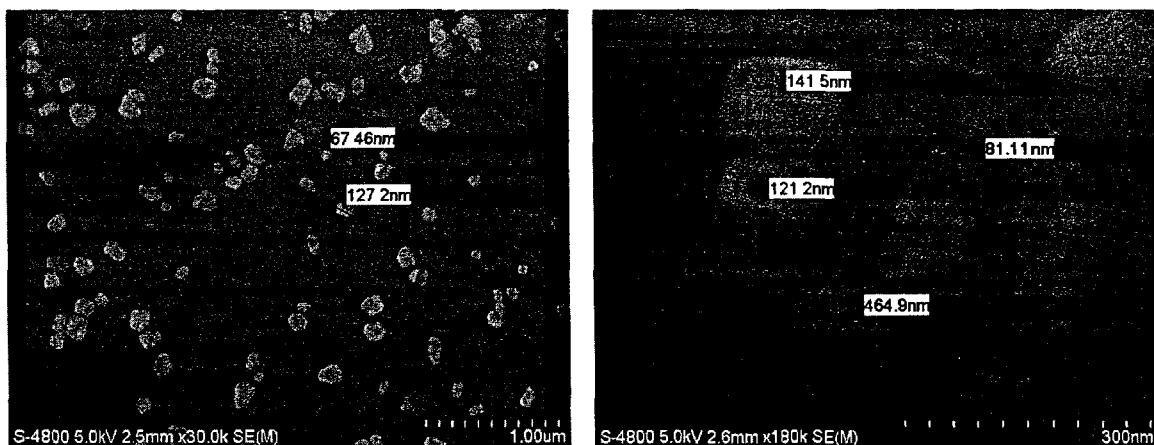
Figure 5-6 SEM image of paclitaxel nanoparticles with shells of
(PS/PSA)$_2$ (left); same sample showing aggregation of
particles at another site (right)

Figures 5-7 shows the SEM images of paclitaxel particles prepared with the
bottom-up approach, then using centrifuge to separate large particles and small
particles.
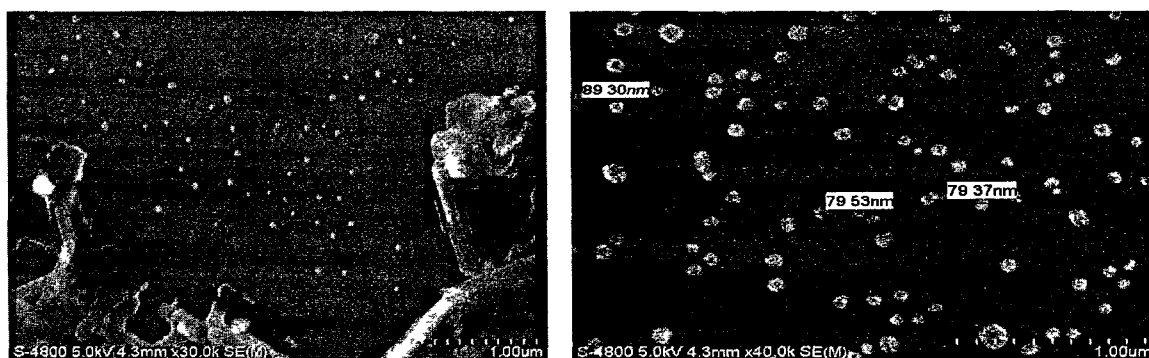
Figure 5-7 SEM image of paclitaxel in 60 % ethanol sonicate for
45 min before (left) and after (right) centrifuge

CHAPTER 6

PROCESS OPTIMIZATION

6.1 Ultrasonication Time

The first parameter we optimized was sonication time It is logical to assume that the longer the sonication, the smaller particles one can get However, in the "top-down" approach, even many hours of sonication did not result in particles less than 200 nm Probably, there is a limitation preventing further splitting of the drug particles In ref [151], it was suggested that this minimal size may be related to the nucleation size of vapor bubbles during sonication The only imporvement which we suggest in future work could be a modification of the cavitation process in sonication by changing solution properties and vapor bubble formation conditions (for example, with increased pressure) Finally, the optimized sonication time for the nanoformulation of curcumin and paclitaxel was chosen to be 30-45 min Another factor, requiring the limitation of sonication time is sample pollution with depleted submicron particles of titanium oxide This pollution is developing with sonication times above one hour and then additional sample purification to eliminate titanium alloy particles is needed Fortunately, it is relatively easy due to different particle densities As shown in Figure 6-1, the particle size decreases when the sonication time increase The result was achieved after seven measurements at each data point The standard deviation was given by the 90Plus particle sizer
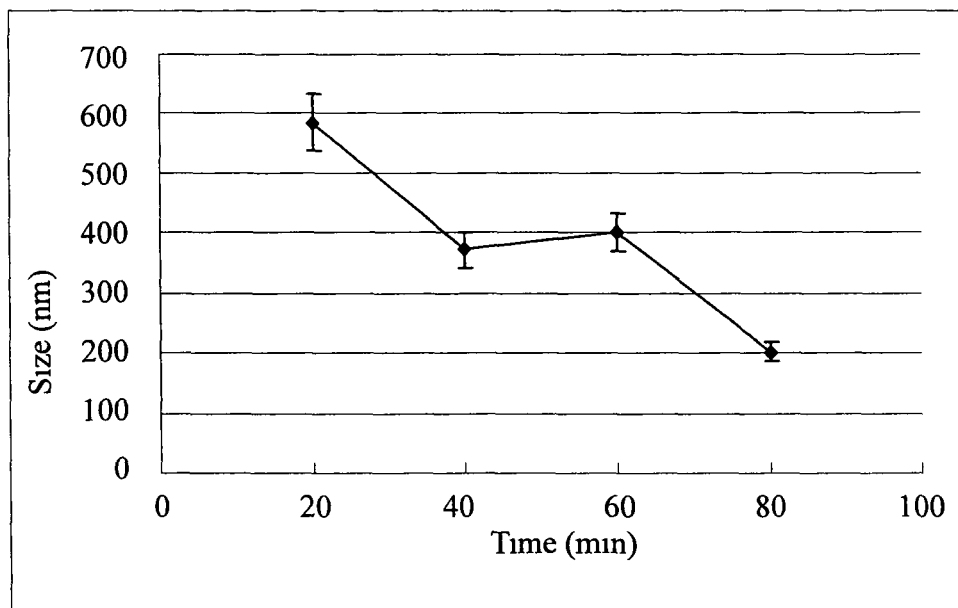
Figure 6-1 Decrease of curcumin nanoparticles size as a function of
sonication time in the presence of polycation Standard
deviation shows the same sample run seven times on
90Plus particle sizer

6.2 Water Add-in Speed and Drug Concentration

To minimize the curcumin particle size, we prepared a series of samples

processed under various conditions (different ethanol/water ratios, drug concentrations,

ultrasonication power, time, and speed of the solvent worsening for crystallization

initiation) Two major factors that affect the crystal size were the rate of water addition

(speed of the solvent worsening) and an initial curcumin concentration These factors

were optimized Figure 6-2 gives the dependence of particle size on the rate of water

addition The result was achieved after seven measurements at each data point The

standard deviation shows the same sample run seven times on 90Plus particle sizer

(Brookhaven Instruments, Co)
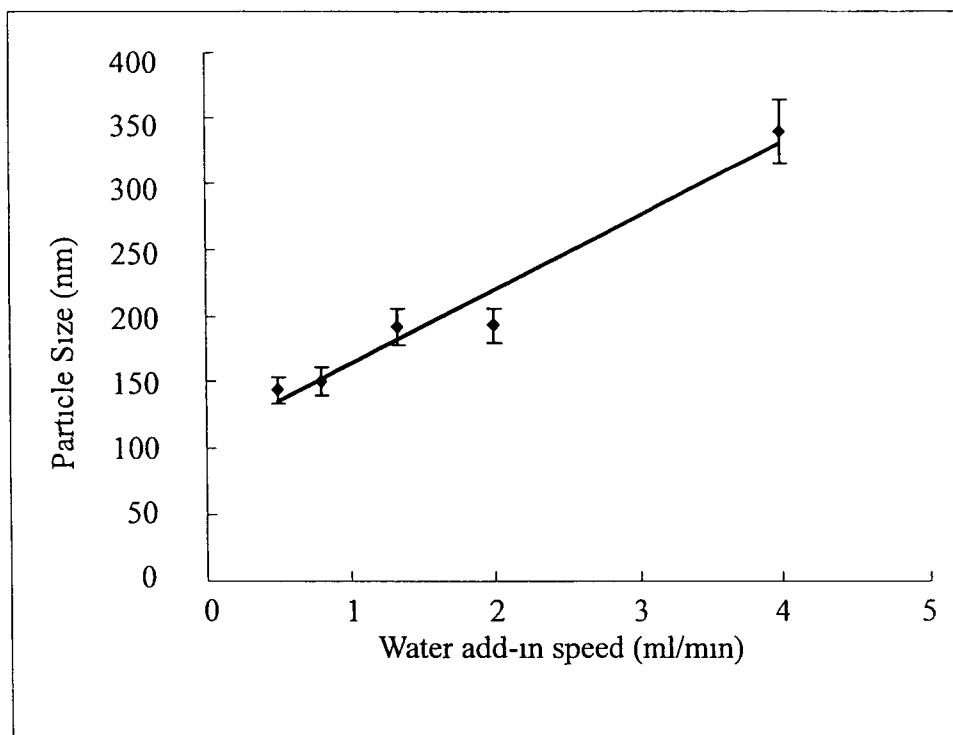
Figure 6-2 Dependence of curcumin particle size on water addition
rate Standard deviation shows the same sample run
seven times on 90Plus particle sizer

The water addition rate was varied from 0 05 mL/min up to 0 4 mL/min for the

sample volume of 50 mL, and the higher rate resulted in the formation of larger

particles We observed particles of ca 320 nm average size at 0 4 mL/min rate versus

ca 120 nm particles for the 0 05 mL/min rate

An increase of curcumin concentration in the initial solution also resulted in

larger nanoparticles as shown in Figure 6-3 The result was achieved after seven

measurements at each data point The standard deviation shows the same sample run

seven times on 90Plus particle sizer (Brookhaven Instruments, Co) Slightly larger

sizes of curcumin nanoparticles, as obtained with the light scattering technique (ca 100

nm) as compared with mean 80 nm size average over thirty particles in the SEM image

may be explained by the fact that light scattering is more sensitive to the admixture of

larger particles in the sample, which were excluded in the SEM estimations [149]
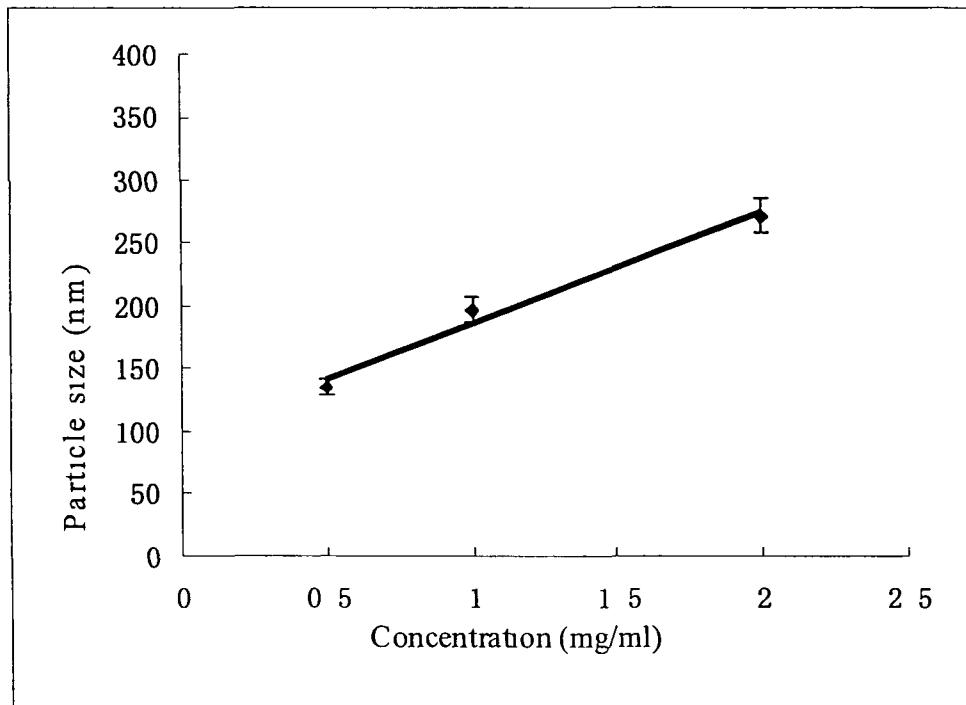
Figure 6-3 Dependence of curcumin particle size on curcumin
concentration Standard deviation shows the same
sample run seven times on 90Plus particle sizer

CHAPTER 7

DRUG RELEASE

We use a set of side-by-side diffusion cells (PermeGear, Inc) to measure the drug release profile

The setup is shown in Figure 7-1 We use a 0 1 μm membrane to separate the two chambers The joint between the sections was sealed with silicone gel We fill the receptor chamber with DI water and fill the donor chamber with the drug sample and start timing After a certain time period we take out all the solution in the receptor chamber and refill it with DI water again Each solution that is taken out from the receptor chamber is labeled (s1, s2,   s(n-1)) then measured for drug concentration with UV spectrophotometer (Agilent 8453) A standard curve is measured earlier to establish the relationship between concentration and absorption, and a linear relationship was found At the end of the release test, both solutions from the receptor chamber (sn) and the donor chamber (sd) were taken out and measured for concentration The release rate was established by accumulating the amount of the drug taken out from the receptor at time x

Total amount of drug =S1+S2+   +Sn+Sd

Release rate at time x= (S1+S2   +Sx) / Total amount of drug
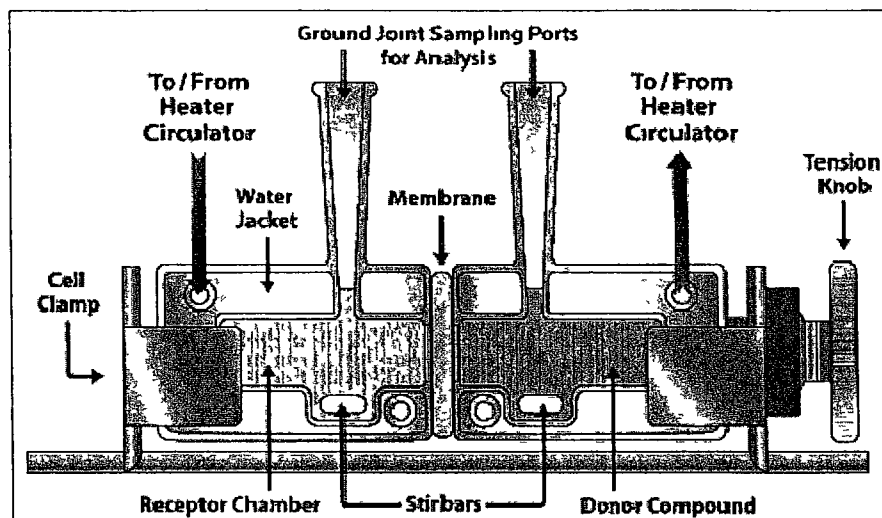
Figure 7-1 Release test side-by-side diffusion cell set up (Scheme
of side-by-side cells kindly provided by PermeGear, Inc)

7 1 Curcumin Release from Nanocapsules

The drug release profile of the curcumin LbL-nanocolloids with the (PS/BSA)$_2$

coating was analyzed in a diffusion chamber (sink conditions) (Figure 7-2) 50 % drug

release from LbL coated nanoparticles was reached in seven hours and 60 % release

was reached within ca 20 hours This release is slower than for nano-curcumin powder

without the LbL shell or the original micronized curcumin We have to emphasize that

the main goal of our work is not slowing down of the drug release rate but the

formulation of stable drug nanocolloids with injectable particle size (below 300 nm)

However, a slower release time is useful and is an indirect proof of the shell formation

providing a diffusion barrier for the particles and slowing down their dissolution
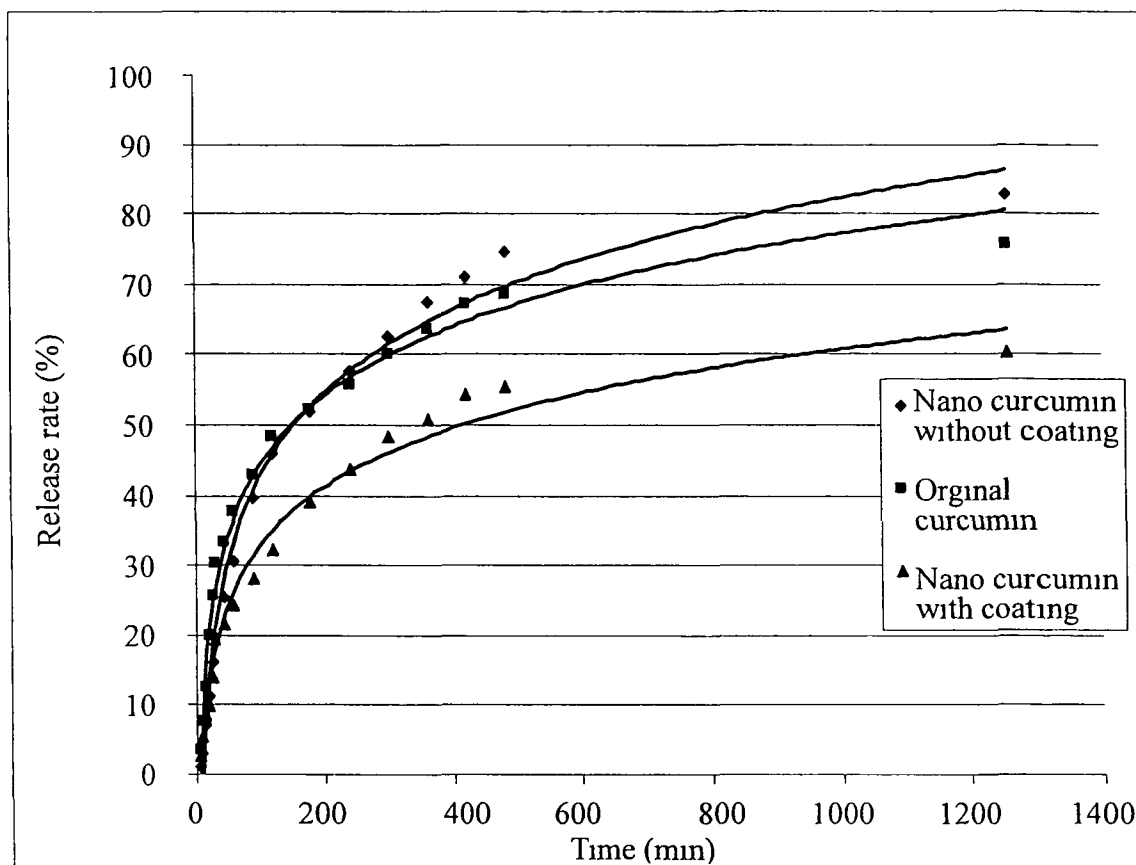
Figure 7-2 Release profiles of curcumin in original micropowder
form, after nanoparticulation and prepared with LbL
nano-encapsulation (the shell composition $(PS/BSA)_2$)

The release profile fits the Peppas model $M_t/M_\infty = Kt^n$, where M_t is the
amount of drug released at time t, M_∞ is the amount of drug released at infinite time, n
is the exponent characteristic of the release mechanism, and K is a constant Detail of
the fitting can be seen in Appendix C The obtained value for n less than 0 5 indicates
that the release mechanism is Fickian diffusion

7.2 Paclitaxel Release from Nanocapsules

The release profiles of the original paclitaxel powder, paclitaxel nanocolloids
with one polycation layer and three polycation/polyanion bilayer coating were analyzed

ın standard sınk condıtıons The fittıng of the release curves were accomplıshed wıth exponentıal Peppas' model Wıthın eıght hours, 70 % of orıgınal paclıtaxel powder was released (Fıgure 7-3)
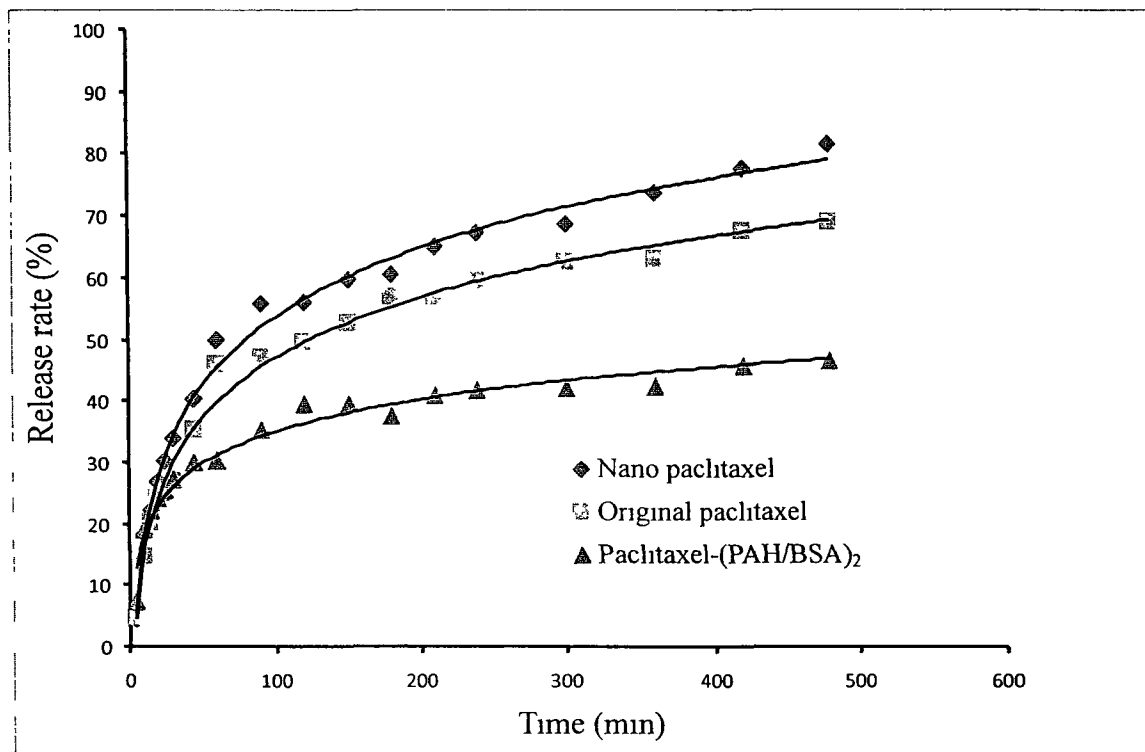
Fıgure 7-3 Release curves for the orıgınal mıcronızed powder of paclıtaxel, uncoated paclıtaxel nanopartıcles (only one PAH layer adsorbed for colloıdal stabılızatıon) and nano-encapsulated paclıtaxel wıth $(PAH/BSA)_2$ shell composıtıon

Nanopartıculated paclıtaxel coated wıth one polyelectrolyte layer leads to slıghtly faster release due to a smaller partıcle sıze ın nanoformulatıon, as compared wıth the mıcrometer sıze of the orıgınal paclıtaxel Paclıtaxel nanocolloıds, coated wıth two bılayers of PAH/BSA, showed a lower drug release rate due to the ıncreasıng thıckness of the capsule wall For example, ın eıght hours, only 40 % of the two layers

coated sample was released as compared with 80 % for the one layer coated sample

The LbL encapsulation technique allows for control of the drug release rate from

polyelectrolytes-stabilized nanoparticles by changes in the number of coating layers or

the shell composition [148]

CHAPTER 8

CONCLUSIONS

Two methods (top-down and bottom-up) of nanoparticle formulation for low water-solubility materials were developed and applied for nanoformulation of anti-cancer drugs curcumin and paclitaxel The resulting drug nanoparticles have a diameter of 100-220 nm and are stable in water

In the first, top-down method, the drug powder was broken up by ultrasound through the collapse of microbubbles (with jet fluid and shock waves) By adding polycations into the solution, the slightly oxidized negative surface of the newly formed particles was recharged positively to a higher surface potential which prevented particles from aggregating This approach was proposed earlier, and we applied it to the new drugs paclitaxel and curcumin, the resulting nanoformulated drug had diameters of ca 200-250 nm

In this work we pioneered the second bottom-up nanoformulation method The drug was dissolved in an organic solvent that is miscible with water (ethanol or acetone) and its nucleation was initiated by the gradual decrease in the solubility of the solution with addition of aqueous polyelectrolyte The process was assisted by ultrasonication Similarly to the first method, the polyelectrolytes coating induced higher surface charge on the formed nanoparticles and provides nanocolloid stability This coating was extended to achieve multilayer encapsulation through alternate adsorption of oppositely

charged synthetic and biodegradable polyelectrolytes (polyallylamine, sodium polystyrenesulfonate, chitosan, bovine serum albumin, protamine sulfate, and alginic acid) Unlike the commonly used emulsion methods, our ultrasonication assisted layer-by-layer nano-encapsulation method allowed for achieving nanoparticles of a much smaller size We obtained crystalline nanoparticles with an average size of 80 nm, and zeta potential of +30 mV or -50 mV (depending on the number of polyelectrolyte layers in the shell), which ensured the stability of the nanocolloids in water for weeks at a concentration of ca 0 2 mg/mL Formation of shells with two bilayers of biocompatible polyelectrolytes allowed for slow drug release during ca 20 hours

The product efficiency of the top-down approach was ca 50 %, which was higher than the efficiency of the bottom-up approach (ca 20 %) The bottom-up approach leads to increased losses due to the formation of larger particles at a fast nucleation rate Larger were removed by centrifugation thus decreasing the yield of the nanoparticles final product

Ultrasound assisted layer-by-layer nano-encapsulation is a promising technique to produce stable 1-2 mg/mL concentration nanocolloids of poor water soluble drugs, like paclitaxel, curcumin, and others The particle size in such drug formulation is reduced from the initial tens of micrometers in the drug powders to 100-200 nm which allow clinical injection Nanoparticle coating with natural polyelectrolytes (polysaccharides) has the potential to increase drug circulation time and availability at a tumor site Layer-by-layer encapsulation was carried out with biodegradable polyelectrolytes protamine sulfate, alginic acid, chitosan and bovine serum albumin The drug particle size can be optimized using either top-down or bottom-up sonicated LbL-treatment

Future work

The stability of nanocolloids at a concentration of 2 mg/mL in buffers with 0 1 M salt concentration needs to be improved Our formulation allowed stable nanocolloids only in solutions with low salt concentrations The free reactive groups of biocompatible polyelectrolytes (amine or acidic) at the outermost layer may help to bind PEG for longer particle circulation in blood or receptors for targeted drug delivery

Further process improvement of both top-down and bottom-up techniques can be achieved by increasing the sonication power Ultrasonication efficiency depends on the shock wave power released on the drug particle surface due to the collapsing of gas microbubbles One can choose additives which will increase the number of bubbles and decompose without damaging the original drug product Another approach to increase sonication power is working under elevated pressure, which may be reached using a compressed gas atmosphere New graduate students will work on constructing a high gas pressure chamber for ultrasonication

For drug nanoparticles targeting, we are planning to use a chemically active layer (with acidic, amine groups) as the outside LbL coating layer to link antibody to target drugs to specific cancer cells

Publications on the dissertation

P Pattekari, Z Zheng, X Zhang, T Levchenko, V Torchilin, Y Lvov, Physical Chemistry, Chemical Physics, v 13, 1624-1629, 2011 "Top-down and bottom-up approach in production aqueous nanocolloids of paclitaxel," journal impact factor 4 1

Z Zheng, X Zhang, D Carbo, C Clark, C-A Nathan, Y Lvov, Langmuir, v 26, 7679-7681, 2010 "Sonication assisted sythesis of polyelectrolyte coated curcumin nanoparticles," journal impact factor 4 1

Ten poster reports at national and international conferences (with published abstracts)

Y Lvov, P Pattekari, X Zhang Z Zheng "Making Aqueous Nanocolloids from Low Soluble Materials LbL Encapsulation," 5th International Conference on Surfaces, Coatings and Nanostructures Materials (NANOSMAT-5), Reims, France, Oct 19-21, 2010

X Zhang, Z Zheng, P Pattekari, Y Lvov "Stable Nanocolloids of Low Soluble Drugs Using Sonication Assisted Layer-by-Layer Technique," Intern   Materials Science & Technology 2010 Conference, Oct 17-21, 2010, Houston

Z Zheng, X Zhang, D Vergara, F Scarlino, M Bukowski, G Giannelli, M Maffia, Y M Lvov, S Leporatti "Nanocarriers for Cancer Therapy - Uptake Visualization " 5th International Conference on Surfaces, Coatings and Nanostructures Materials (NANOSMAT-5), Reims, France, Oct 19-21, 2010

Z Zheng, X Zhang, Y Lvov, G Giovinazzo, A Santino, S Leporatti "Nanocapsules for Cancer Therapy," Particles 2010 - Medical, Pharmaceutical, and Drug Delivery Applications, International Conference, 22-25 May 2010, Lake Buena Vista, FL

Y Lvov, V Torchilin, X Zhang, Z Zheng, P Pattekari "100-nm Diameter Colloidal Particles of Poorly Soluble Anti-Cancer Drugs Prepared by LbL Encapsulation," 13th International Conference on Organized Molecular Films (LB-13), July 18-21, 2010, Quebec City, Canada

V Vergaro, I Palama, Z Zheng, R Cingolani, Y Lvov, S Leporatti "Cytomechanical modifications induced by drug-loaded carriers uptake by breast cancer cells " 2009 European Biophysical Society Meeting, Genova, Italy, July 11-15, 2009

Z Zheng, Y Lvov, G Giovinazzo, A Santino, R Cingolani, R Rinaldi, S Leporatti "Cytomechanical and morphological modifications of cancer cells induced by drug-carriers A Scanning Force Microscopy (SFM) study " Nanoscale-VII Veeco Intern Conference, Santa Barbara, July 28-31, 2009

Y Lvov, E Abdullayev, Z Zheng "Smart nanocontainers for delivery of chemical agents Architectural capsules and tubes," 83rd ACS Colloid & Surface Science Symposium and 13th Intern Conference on Surface Science, New York, June 16, 2009

S Madisetti, Z Zheng, Z Gong, S Penmetsa, Y Lvov, L Que "Layer-by-Layer Nanoscale Coating of Microparticles with Droplet Microfluidic Device," 4th Annual International Conference on Nano, Micro Engineering and Molecular Systems, IEEE-NEMS'09, Shenzhen, China, Jan 8-12, 2009

Z Zheng, D Carbo, C -A Nathan, Y Lvov "Sonicated Assisted LbL Assembly of Nanocapsules," 264 Southwest Regional American Chemical Society Meeting, Little Rock, Oct 1-4, 2008

Patents and disclosures based on this work

US patent application by V Torchilin, Y Lvov, Z Zheng "Stable Aqueous Nanocolloids of Paclitaxel and Atavoquone," jointly filed by Louisiana Tech University and Northeastern University on April 25, 2009

LaTech disclosures

1) Z Zheng, Y Lvov "Sonication synthesis of polyelectrolyte coated nanoparticles through mixing molecular solutions with bad solvents," September 30, #2008-27

2) Y Lvov, Z Zheng, V Torchilin "Paclitaxel and atavoquone nanoparticles production through ultrasonication with gradual desolvation assisted with polycation coating Synthesis of the mixed drugs nanoparticles," December 1, #2008-30

APPENDIX A

POLYELECTROLYTE REQUIRED FOR NO-WASH PROCESS

To estimate the minimum amount of polyelectrolyte needed for complete coverage of nanoparticles we perform the calculation in Table A-1 In this case we calculate the PAH needed to complete coat 2 g of paclitaxel which have a rectangular sharp and average edge of 300 nm length

Table A-1 Minimum amount of polyelectrolyte needed for coating

Assume PTX density=	1 5	g/cm^3
PTX weight	2 00E-02	g
average single PTX size	3 00E-05	cm
average single PTX size nm	3 00E+02	nm
volume of PTX=w/p	1 3333E-02	cm^3
single PTX volume	2 70E-14	cm^3
number of PTX particle	4 9383E+11	
single PTX surface	5 40E-09	cm^2
total surface	2 6667E+03	cm^2
thickness of PAH	2 00E-07	cm
thickness of PAH nm	2 00E+00	nm
volume of PAH	5 3333E-04	cm^3
PAH density	1 6	g/cm^3
PAH weight	8 5333E-04	g
PAH weight in mg	8 5333E-01	mg

APPENDIX B

NANOCOLLOID PARTICLE DISTANCE CALCULATION

We found that the stability of drug nano colloid was effect by the concentration of the colloid In general, we found the lower the concentration the better the stability To estimate the average distance between particles at a certain concentration, we prefer the calculation in Table B-1 (for sphere sharp) and Table B-2 (for cube sharp)

Table B-1 Average distance between sphere particles

Calculate particle as sphere	Sample 1	Sample 2	Sample 3
Weight of drug in 1ml solution(mg)	0 5	2	5
Density of drug (mg/ml)	1500	1500	1500
Weight of water (mg)	1000	1000	1000
Concentration (mg/ml)	0 5	2	5
Size of particles (nm)	200	200	200
Size of particles (cm)	0 00002	0 00002	0 00002
Weight of each particle (mg)	6 28E-12	6 28E-12	6 28E-12
Number of particles	7 96E+10	3 18E+11	7 96E+11
Volume of each particle (round) (ml)	4 19E-15	4 19E-15	4 19E-15
Volume of solution outside a particle(ml)	1 26E-11	3 14E-12	1 26E-12
Volume of each cell (ml)	1 26E-11	3 15E-12	1 26E-12
Distantce cm	0 000232	0 000146	0 000108
Distantce μm	2 324897	1 464593	1 079121

Table B-2 Average distance between cube particles

Calculate particle as cube	Sample 1	Sample 2	Sample 3
Weight of drug in 1ml solution(mg)	0 5	2	5
Density of drug (mg/ml)	1500	1500	1500
Weight of water (mg)	1000	1000	1000
Concentration (mg/ml)	0 5	2	5
Size of particles (nm)	200	200	200
Size of particles (cm)	0 00002	0 00002	0 00002
Weight of each particle (mg)	1 2E-11	1 2E-11	1 2E-11
Number of particles	4 17E+10	1 67E+11	4 17E+11
Volume of each particle (cube) (ml)	8E-15	8E-15	8E-15
Volume of solution outside a particle (ml)	2 4E-11	6E-12	2 4E-12
Volum of each cell (ml)	2 4E-11	6 01E-12	2 41E-12
Distantce cm	0 000288	0 000182	0 000134
Distantce μm	2 884499	1 817121	1 338866

To show the result in 3D image we use Matlab 2007 to plot the image The program code is shown below

```
%nanoparticles size and distance calculation

%written by zhiguo zheng

%PhD student of Biomedical Engineering of Louisiana Tech University%

clc

clear all

%draw 3d sphere radius r nm in s nm cube cell

[xsp,ysp,zsp] = sphere(20),

r=200,

d=1079,

s=2000,

xsp=xsp *r,

ysp=ysp *r,

zsp=zsp *r,

for i = -s d s,

    for j=-s d s,

        for k=-s d s,

            surface(xsp+i,ysp+j,zsp+k),

        end

    end,

end,

axis equal,

view([50,20]),
```

The simulation results for 200 nm sphere paclitaxel nanoparticles at concentration of

0 5 and 5 mg/mL are shown in Figure B-1
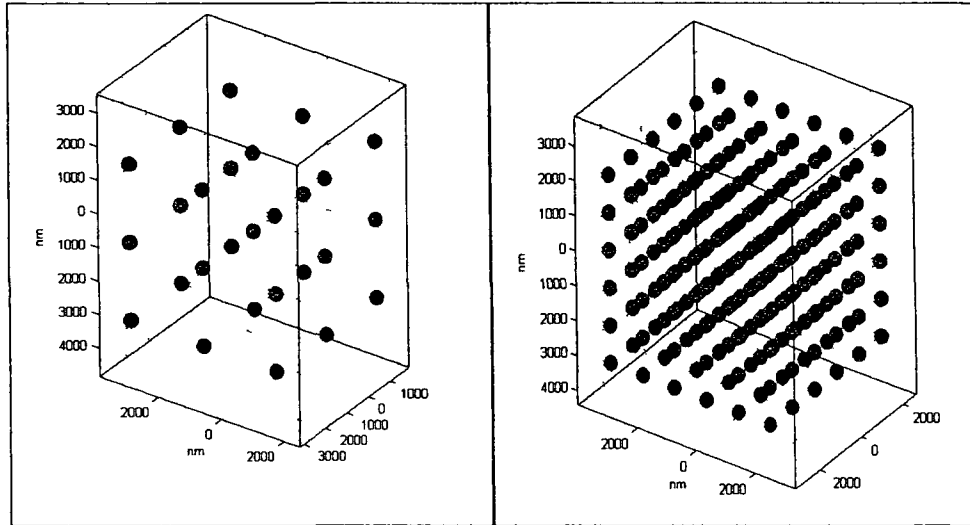
Figure B-1 Simulation for 200 nm sephere sharp paclitaxel
concentration at 0 5 mg/mL (left) and 5 mg/mL (right)

%nanoparticles size and distance calculation

%written by zhiguo zheng

%PhD student of Biomedical Engineering of Louisiana Tech University

clc, clear all,

%draw 3d cubes edge length r nm in distance d nm in a s nm cube cell

x=[0 1 1 0 0 0,1 1 0 0 1 1,1 1 0 0 1 1,0 1 1 0 0 0],

y=[0 0 1 1 0 0,0 1 1 0 0 0,0 1 1 0 1 1,0 0 1 1 1 1],

z=[0 0 0 0 0 1,0 0 0 0 0 1,1 1 1 1 0 1,1 1 1 1 0 1],

r=200,

d=1339,

s=3000,

x=x *r,

y=y *r,

z=z *r,

for i = -s d s,

    for j=-s d s,

        for k=-s d s,

            surface(x+i,y+j,z+k),

        end,

    end,

end,

axis equal,

view([35,30]),

The simulation results for 200 nm cube sharp paclitaxel nanoparticles at concentration of 0 5 and 5 mg/mL are shown in Figure B-2
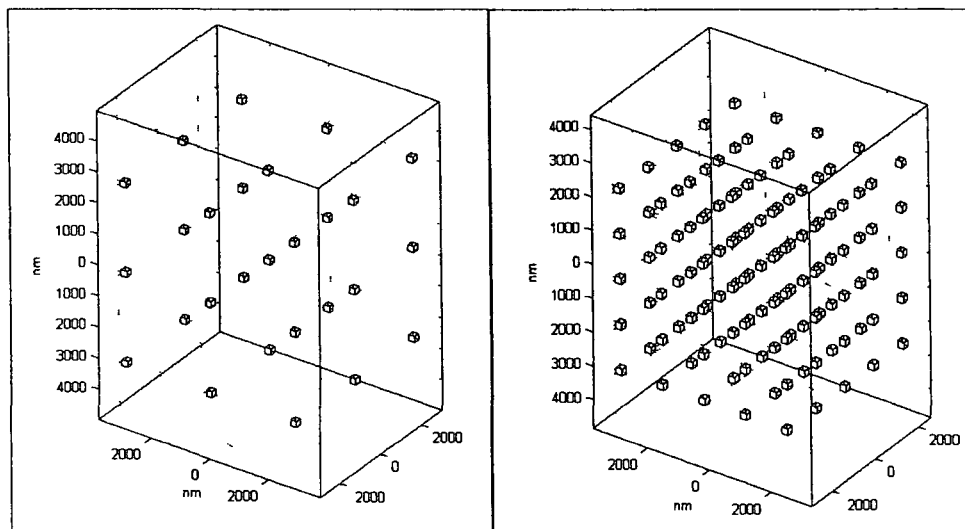
Figure B-2 Simulation for 200 nm cube sharp paclitaxel
concentration at 0 5 mg/mL (left) and 5 mg/mL (right)

APPENDIX C

RELEASE MODEL FITTING

For release curve in Figure 7-2 we use OriginPro 8 1 software to fit the experiment data with moding equation

In this study, we use Ritger-Peppas' empirical Equation

$$\frac{M_t}{M_\infty} = kt^n$$

Figure C-1 shows the fitting of experiment result using Ritger-Peppas' empirical equation The fitting results are shown in Table C-1

Table C-1 Fitting results for the curcumin release profile

Model	Ritger-Peppas		
Equation	$y = a*x^b$		
Reduced Chi-Sqr	3 48E-04	1 80E-04	4 49E-04
Adj R-Square	0 99468	0 99455	0 99019
		Value	Standard error
Nano curcumin	a	0 34387	0 10581
Nano curcumin	b	0 21044	0 03356
Orginal curcumin	a	11 00387	37 90579
Orginal curcumin	b	0 01274	0 04171
Curcumin/(PS/BSA)$_2$	a	0 18261	0 05416
Curcumin/(PS/BSA)$_2$	b	0 24341	0 0346
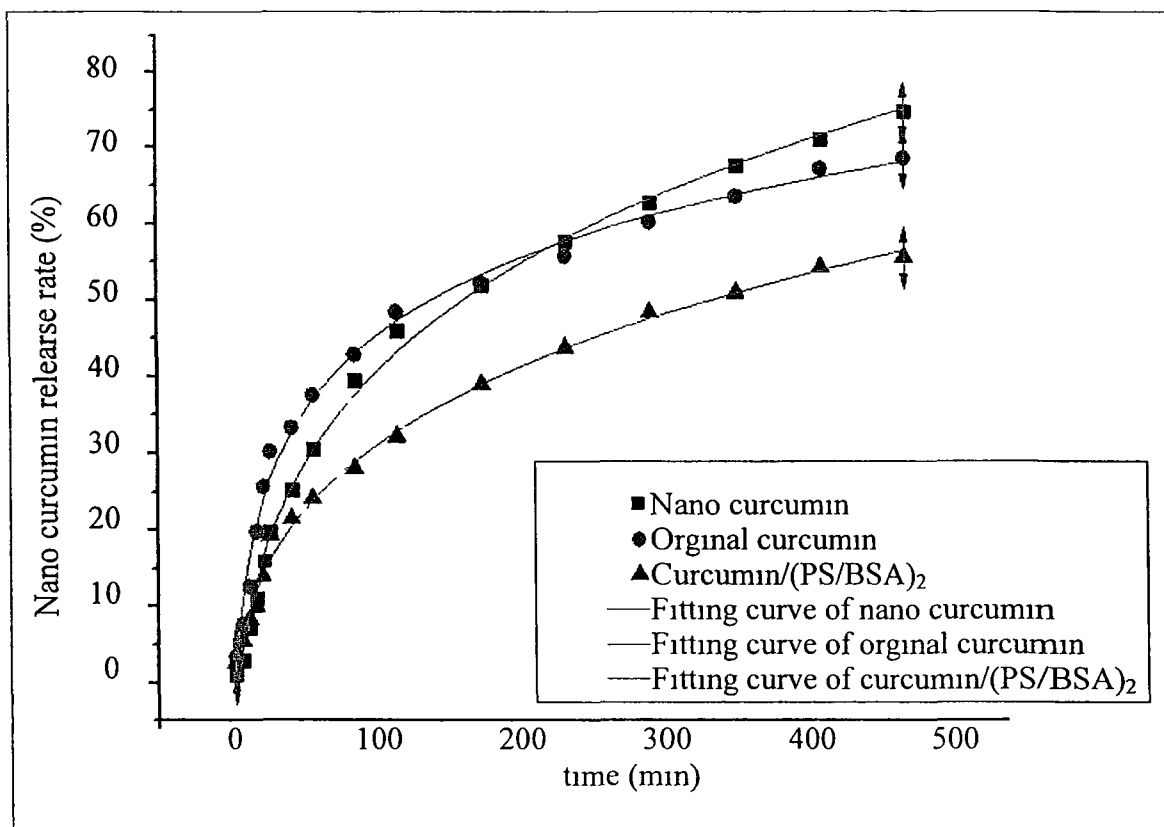
Figure C-1 Fitting result for curcumin release

Figure C-2 shows the fitting of experiment result using Ritger-Peppas' empirical

equation The fitting results are shown in Table C-2

Table C-2 Fitting results for the paclitaxel release profile

Model	Ritger-Peppas		
Equation	$Y = a*x^b$		
Reduced Chi-Sqr	5 35939	4 71E+00	2 45E+00
Adj R-Square	0 93758	0 93513	0 9103
		Value	Standard Error
Nano paclitaxel	a	10 72209	1 38742
Nano paclitaxel	b	0 33469	0 02507
Orginal paclitaxel	a	9 46E+00	1 27E+00
Orginal paclitaxel	b	0 33125	0 02535
Paclitaxel/(PAH/BSA)$_2$	a	11 31214	1 30579
Paclitaxel/(PAH/BSA)$_2$	b	0 23387	0 02159
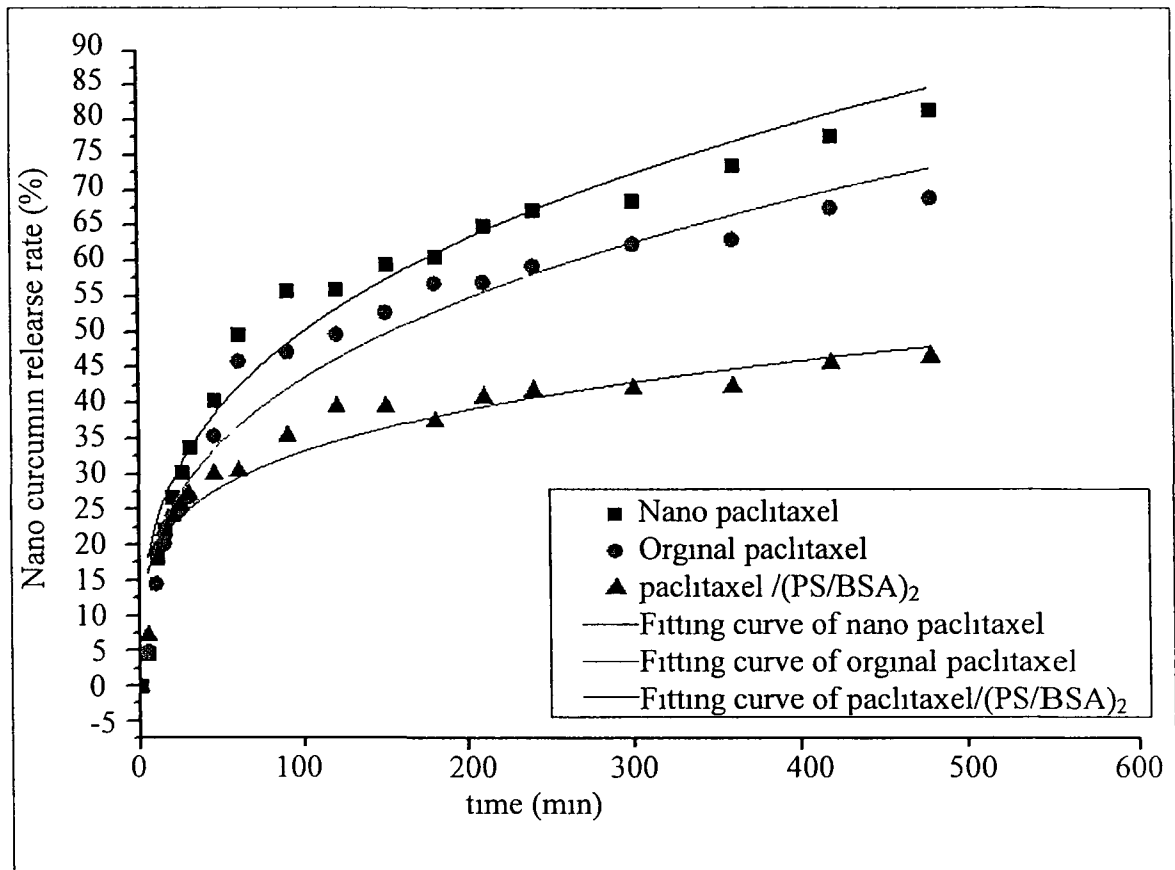
Figure C-2 Fitting result for paclitaxel release

BIBLIOGRAPHY

[1] S F Altekruse, C L Kosary, M Krapcho, N Neyman, R Aminou, W Waldron, J Ruhl, N Howlader, Z Tatalovich, H Cho, A Mariotto, M P Eisner, D R Lewis, K Cronin, H S Chen, E J Feuer, D G Stinchcomb, B K Edwards (eds) "SEER Cancer Statistics Review, 1975-2007," National Cancer Institute, 2009, pp 5-6

[2] R R H Coombs, D W Robinson (eds) "Nanotechnology in Medicine and the Biosciences," Series *Development in Nanotechnologies*, Gordon and Breach Publishers, 1996, pp 3-16

[3] E Yaghini, A M Seifalian, A J MacRobert "Quantum dots and their potential biomedical applications in photosensitization for photodynamic therapy," *Nanomedicine*, vol 4, pp 353-363, 2009

[4] H Maeda "SMANCS and polymer-conjugated macromolecular drugs Advantages in cancer chemotherapy," *Adv Drug Delivery Rev*, vol 46, pp 169-185, 2001

[5] A K Iyer, G Khaled, J Fang, H Maeda "Exploiting the enhanced permeability and retention effect for tumor targeting," *Drug Discovery Today*, vol 11, pp 812-818, 2006

[6] M Gaumet, A Vargas, R Gurny, F Delie "Nanoparticles for drug delivery The need for precision in reporting particle size parameters," *Eur J Pharm Biopharm*, vol 69, pp 1-9, 2008

[7]   D E Owens, N A Peppas "Opsonization, biodistribution, and pharmaco-
        kinetics of polymeric nanoparticles," *Int J Pharm*, vol 307, pp 93-102,
        2006

[8]   S Nagayama, K Ogawara, Y Fukuoka, K Higaki, T Kimura "Time-
        dependent changes in opsonin amount associated on nanoparticles alter their
        hepatic uptake characteristics," *Int J Pharm*, vol 342, pp 215-221, 2007

[9]   A S Hoffman "The origins and evolution of 'controlled' drug delivery
        systems," *J Control Release*, vol 132, pp 153-163, 2008

[10]   S M Janib, A S Moses, J A MacKay "Imaging and drug delivery using
        theranostic nanoparticles," *Adv Drug Delivery Rev*, vol 62, pp 1052-1063,
        2010

[11]   M J Hawkins, P Soon-Shiong, N Desai "Protein nanoparticles as drug
        carriers in clinical medicine," *Adv Drug Deliv Rev*, vol 60, pp 876-885,
        2008

[12]   A Gaitanis, S Staal "Liposomal doxorubicin and nab-paclitaxel
        Nanoparticle cancer chemotherapy in current clinical use," *Methods Mol
        Biol*, vol 624, pp 385-392, 2010

[13]   E Miele, G P Spinelli, F Tomao, S Tomao "Albumin-bound formulation of
        paclitaxel (Abraxane ABI-007) in the treatment of breast cancer," *Int
        J Nanomedicine*, vol 4, pp 99-105, 2009

[14]   M J Hawkins, P Soon-Shiong, N Desai "Protein nanoparticles as drug
        carriers in clinical medicine," *Adv Drug Deliv Rev*, vol 60, pp 876-885,
        2008

[15]   K Uekama "Design and evaluation of cyclodextrin-based drug formulation,"
         Chem Pharm Bull , vol 52, pp 900-915, 2004

[16]   M E Davis, M E Brewster "Cyclodextrin-based pharmaceutics Past, present
         and future," *Nat Rev Drug Discovery*, vol 3, pp 1023-1035, 2004

[17]   A Surendiran, S Sandhiya, S C Pradhan, C Adithan "Novel applications of
         nanotechnology in medicine," *Indian J Med Res* , vol 130, pp 689-701,
         2009

[18]   C C Lee, J A MacKay, J M Frechet, F C Szoka "Designing dendrimers for
         biological applications," *Nat Biotechnol* , vol 23, pp 1517-1526, 2005

[19]   R G Strickley "Solubilizing excipients in oral and injectable formulations,"
         Pharm Res , vol 21, pp 201-230, 2004

[20]   K Kawakami, K Miyoshi, Y Ida "Solubilization behavior of poorly soluble
         drugs with combined use of Gelucire 44/14 and cosolvent," *J Pharm Sci* ,
         vol 93, pp 1471-1479, 2004

[21]   K Kawakami, N Oda, K Miyoshi, T Funaki, Y Ida "Solubilization behavior
         of a poorly soluble drug under combined use of surfactants and cosolvents,"
         Eur J Pharm Sci , vol 28, pp 7-14, 2006

[22]   J Liu, H Lee, C Allen "Formulation of drugs in block copolymer micelles
         Drug loading and release," *Curr Pharm Des* , vol 12, pp 4685-4701, 2006

[23]   V P Torchilin "Micellar nanocarriers Pharmaceutical perspectives," *Pharm
         Res* , vol 24, pp 1-16, 2007

[24]   Y Kakizawa, K Kataoka "Block copolymer micelles for delivery of gene
         and related compounds," *Adv Drug Delivery Rev* , vol 54, pp 203-222,
         2002

[25] M R Kano, Y Bae, C Iwata, Y Morishita, M Yashiro, M Oka, Y Fujii, A Komuro, K Kiyono, M Kaminishi, K Hirakawa, Y Ouchi, N Nishiyama, K Kataoka, K Miyazono "Improvement of cancer-targeting therapy, using nanocarriers for intractable solid tumors by inhibition of TGF signaling," *Proc Natl Acad Sci USA*, vol 104, pp 3460-3465, 2007

[26] N Nishiyama, A Iriyama, W D Jang, K Miyata, K Itaka, Y Inoue, H Takahashi, Y Yanagi, Y Tamaki, H Koyama, K Kataoka "Light-induced gene transfer from packaged DNA enveloped in a dendrimeric photosesnsitizer," *Nat Materials*, vol 4, pp 934-941, 2005

[27] V P Torchilin "Targeted polymeric micelles for delivery of poorly soluble drugs," Cell Mol Life Sci , vol 61, pp 2549-2559, 2004

[28] M Talelli, C J Rijcken, C F van Nostrum, G Storm, W E Hennink "Micelles based on HPMA copolymers," *Adv Drug Deliv Rev* , vol 62, pp 231-239, 2010

[29] N Nasongkla, E Bey, J Ren, H Ai, C Khemtong, J S Guthi, S F Chin, A D Sherry, D A Boothman, J Gao "Multifunctional polymeric micelles as cancer-targeted, MRI-ultrasensitive drug delivery systems," Nano Lett , vol 6, pp 2427-2430, 2006

[30] S C Kim, D W Kim, Y H Shim, J S Bang, H S Oh, S Wan Kim, M H Seo "In vivo evaluation of polymeric micellar paclitaxel formulation Toxicity and efficacy," *J Control Release*, vol 72, pp 191-202, 2001

[31]   K S Lee, H C Chung, S A Im, Y H Park, C S Kim, S B Kim, S Y Rha, M Y Lee, J "Multicenter phase II trial of Genexol-PM, a Cremophor-free, polymeric micelle formulation of paclitaxel, in patients with metastatic breast cancer," *Breast Cancer Res Treat*, vol 108, pp 241-250, 2008

[32]   D W Kim, S Y Kim, H K Kim, S W Kim, S W Shin, J S Kim, K Park, M Y Lee, D S "Multicenter phase II trial of Genexol-PM, a novel Cremophor-free, polymeric micelle formulation of paclitaxel, with cisplatin in patients with advanced non-small-cell lung cancer," *Ann Oncol*, vol 18, pp 2009-2014, 2007

[33]   W T Lim, E H Tan, C K Toh, S W Hee, S S Leong, P C Ang, N S Wong, B Chowbay "Phase I pharmacokinetic study of a weekly liposomal paclitaxel formulation (Genexol-PM) in patients with solid tumors," *Ann Oncol*, vol 21, pp 382-388, 2010

[34]   M Talelli, C J Rijcken, C F van Nostrum, G Storm, W E Hennink "Micelles based on HPMA copolymers," *Adv Drug Deliv Rev*, vol 62, pp 231-239, 2010

[35]   N Nasongkla, E Bey, J Ren, H Ai, C Khemtong, J S Guthi, S F Chin, A D Sherry, D A Boothman, J Gao "Multifunctional polymeric micelles as cancer-targeted, MRI-ultrasensitive drug delivery systems," Nano Lett, vol 6, pp 2427-2430, 2006

[36]   S C Kim, D W Kim, Y H Shim, J S Bang, H S Oh, S Wan Kim, M H Seo "In vivo evaluation of polymeric micellar paclitaxel formulation Toxicity and efficacy," *J Control Release*, vol 72, pp 191-202, 2001

[37]   K S Lee, H C Chung, S A Im, Y H Park, C S Kim, S B Kim, S Y Rha, M Y Lee, J "Multicenter phase II trial of Genexol-PM, a Cremophor-free, polymeric micelle formulation of paclitaxel, in patients with metastatic breast cancer," *Breast Cancer Res Treat*, vol 108, pp 241-250, 2008

[38]   D W Kim, S Y Kim, H K Kim, S W Kim, S W Shin, J S Kim, K Park, M Y Lee, D S "Multicenter phase II trial of Genexol-PM, a novel Cremophor-free, polymeric micelle formulation of paclitaxel, with cisplatin in patients with advanced non-small-cell lung cancer," *Ann Oncol*, vol 18, pp 2009-2014, 2007

[39]   W T Lim, E H Tan, C K Toh, S W Hee, S S Leong, P C Ang, N S Wong, B Chowbay "Phase I pharmacokinetic study of a weekly liposomal paclitaxel formulation (Genexol-PM) in patients with solid tumors," *Ann Oncol*, vol 21, pp 382-388, 2010

[40]   Y Barenholz "Liposome application Problems and prospects," *Curr Opin Colloid Interface Sci*, vol 6, pp 66-77, 2001

[41]   K Kogure, H Akita, Y Yamada, H Harashima "Multifunctional envelope-type nano device (MEND) as a non-viral gene delivery system," *Adv Drug Delivery Rev*, vol 60, pp 559-571, 2008

[42]   V P Torchilin "Recent advances with liposomes as pharmaceutical carriers," *Nat Rev Drug Discov*, vol 4, pp 145-160, 2005

[43]   D H Levine, P P Ghoroghchian, J Freudenberg, G Zhang, M J Therien, M I Greene, D A Hammer, R Murali "Polymersomes A new multi-functional tool for cancer diagnosis and therapy," *Methods*, vol 46, pp 25-32, 2008

[44]   P P Adiseshaiah, J B Hall, S E McNeil "Nanomaterial standards for efficacy and toxicity assessment," *Wiley Interdiscip Rev Nanomed Nanobiotechnol* , vol 2, pp 99-112, 2010

[45]   A Gaitanis, S Staal "Liposomal doxorubicin and nab-paclitaxel Nanoparticle cancer chemotherapy in current clinical use," *Methods Mol Biol* , vol 624, pp 385-392, 2010

[46]   S Liu, M Y Han "Silica-coated metal nanoparticles," *Chem Asian J* , vol 5, pp 36-45, 2010

[47]   A Wei, A P Leonov, Q Wei "Gold nanorods Multifunctional agents for cancer imaging and therapy," *Methods Mol Biol* , vol 624, pp 119-130, 2010

[48]   K Sokolov, J Tam, K Travis, T Larson, J Aaron, N Harrison, S Emelianov, K Jo "Cancer imaging and therapy withmetal nanoparticles," *Conf Proc IEEE Eng Med Biol Soc 2009*, pp 2005-2007

[49]   M Ao, Z Wang, H Ran, D Guo, J Yu, A Li, W Chen, W Wu and Y Zheng "Gd-DTPA-loaded PLGA microbubbles as both ultrasound contrast agent and MRI contrast agent—a feasibility research," *J Biomed Mater Res B Appl Biomater* , vol 93, pp 551-556, 2010

[50]   S J Lee, J R Jeong, S C Shin, J C Kim, Y H Chang, Y M Chang, J D Kim "Nanoparticles ofmagnetic ferric oxides encapsulated with poly(D, L latide-co-glycolide) and their applications to magnetic resonance imaging contrast agent," *J Magn Magn Mater* , vol 272-76, pp 2432-2433, 2004

[51]   S J Son, X Bai, S B Lee "Inorganic hollow nanoparticles and nanotubes in nanomedicine part 1 drug/gene delivery applications," *Drug Discovery Today*, vol 12, pp 650-656, 2007

[52]   I I Slowing, J L Vivero-Escoto, C W Wu, V S Y Lin "Mesoporous silica nanoparticles as controlled release drug delivery and gene transfection carriers," *Adv Drug Delivery Rev* , vol 60, pp 1278-1288, 2008

[53]   C Y Lai,   B G Trewyn,   D M Jeftinija,   K Jeftinija,   S Xu,   S Jeftinija, V S Y Lin "A mesoporous silica nanosphere-based carrier system with chemically removable CdS nanoparticle caps for stimuli-responsive controlled release of neurotransmitters and drug molecules," *J Am Chem Soc* , vol 125, pp 4451-4459, 2003

[54]   K Ariga, A Vinu, M Miyahara, J P Hill, T Mori "One-pot separation of tea components through selective adsorption on pore-engineered nanocarbon, carbon nanocage," *J Am Chem Soc* , vol 129, pp 11022-11023, 2007

[55]   K Ariga, A Vinu, Q Ji, O Ohmori, J P Hill, S Acharya, J Koike, S Shiratori "A layered mesoporous carbon sensor based on nanopore-filling cooperative adsorption in the liquid phase," *Angew Chem Int Ed* , vol 47, pp 7254-7257, 2008

[56]   I Roy, S Mitra, A Maitra, S Mozumdar "Calcium phosphate nanoparticles as novel non-viral vectors for targeted gene delivery," *Int J Pharm* , vol 250, pp 25-33, 2003

[57]   P Horcajada, C Serre, G Maurin, N A Ramsahye, F Balas, M Vallet-Regi M Sebban, F Taulelle, G Ferey "Flexible porous metal-organic frameworks for a controlled drug delivery," *J Am Chem Soc* , vol 130, pp 6774-6780, 2008

[58]   A Gaitanis, S Staal "Liposomal doxorubicin and nab-paclitaxel Nanoparticle cancer chemotherapy in current clinical use," *Methods Mol Biol* , vol 624, pp 385-392, 2010

[59]   M R Dreher, D Raucher, N Balu, O Michael Colvin, S M Ludeman "Evaluation of an elastin-like polypeptide-doxorubicin conjugate for cancer therapy," *J Control Release*, vol 91, pp 31-43, 2003

[60]   D Y Furgeson, M R Dreher "Structural optimization of a 'smart' doxorubicin-polypeptide conjugate for thermally targeted delivery to solidtumors," *J Control Release*, vol 110, pp 362-369, 2006

[61]   G L Bidwell III, A N Davis, I Fokt, W Priebe, D Raucher "A thermally targeted elastin-like polypeptide-doxorubicin conjugate overcomes drug resistance," *Invest New Drugs*, vol 25, pp 313-326, 2007

[62]   L Dennany, P Sherrell, J Chen, P C Innis, G G Wallace, A I Minett "Epr characterisation of platinum nanoparticle functionalised carbon nanotube hybrid materials," *Phys Chem Chem Phys* , vol 12, pp 4135-4141, 2010

[63]   S Dhar, Z Liu, J Thomale, H Dai, S J Lippard "Targeted single-wall carbonnanotube-mediated Pt(IV) prodrug delivery using folate as a homing device," *J Am Chem Soc* , vol 130, pp 11467-11476, 2008

[64]   A A Bhirde, V Patel, J Gavard, G Zhang, A A Sousa, A Masedunskas, R D Leapman, R Weigert, J S Gutkind, J F Rusling "Targeted killing of cancer cells in vivo and in vitro with EGF-directed carbon nanotube-based drug delivery," *ACS Nano*, vol 3, pp 307-316, 2009

[65]   A A Shvedova, V E Kagan "The role of nanotoxicology in realizing the 'helping without harm' paradigm of nanomedicine Lessons from studies of pulmonary effects of single-walled carbon nanotubes," *J Intern Med*, vol 267, pp 106-118, 2010

[66]   C Sanchez-Cano, M J Hannon "Novel and emerging approaches for the delivery of metallo-drugs," *Dalton Trans*, pp 10702-10711, 2009

[67]   K L Aillon, Y Xie, N El-Gendy, C J Berkland, M L Forrest "Effects of nanomaterial physicochemical properties on in vivo toxicity," *Adv Drug Deliv Rev*, vol 61, pp 457-466, 2009

[68]   R Price, B Gaber, Y Lvov "In-vitro release characteristics of tetracycline, khellin and nicotinamide adenine dinucleotide from halloysite, a cylindrical mineral for delivery of biologically active agents," *J Microencapsulation*, vol 18, pp 713-723, 2001

[69]   N Veerabadran, R Price, Y Lvov "Clay nanotubules for drug encapsulation and dustained release," *ACS Nano J*, vol 2, pp 215-222, 2007

[70]   Y Lvov, D Shchukin, H Mohwald, R Price "Clay nanotubes for controlled release of protective agents," *ACS Nano J*, vol 2, pp 814-820, 2008

[71]   N Veerabadran, Y Lvov, R Price "Organized shells on clay nanotubes for controlled release of macromolecules," *Macromolecular Rapid Commun*, vol 24, pp 99-103, 2009

[72]   V Vergaro,   E Abdullayev,   R Cingolani,   Y Lvov,   S Leporatti
"Citobiocompatibility and uptake for clay nanotubes," *Biomacromolecules*,
vol 11, pp 820-229, 2010

[73]   K Ariga, J P Hill, Q Ji "Layer-by-layer assembly as a versatile bottom-up
nanofabrication technique for exploratory research and realistic application,"
Phys Chem Chem Phys , vol 9, pp 2319-2340, 2007

[74]   K Ariga, J P Hill, Q Ji "Biomaterials and biofunctionality in layered
macromolecular assemblies," *Macromol Biosci* , vol 8, pp 981-990, 2008

[75]   R K Iler "Multilayers of colloidal particles," *J Colloid Interface Sci* ,
vol 21, pp 569-594, 1966

[76]   G Decher, J D Hong "Buildup of ultrathin multilayer films by a self-
assembly process 1 Consecutive adsorption of anionic and cationic bipolar
amphiphile on charged surfaces," *Macromol Chem Macromol Symp* ,
vol 46, pp 321-327, 1991

[77]   G Decher "Fuzzy nanoassemblies Toward layered polymeric multi-
composites," *Science*, vol 277, pp 1232-1237, 1997

[78]   S W Keller, H Kim, T E Mallouk "Layer-by-layer assembly of interaction
compound and heterostructures on surfaces Toward molecular beaker
epitaxy," *J Am Chem Soc* , vol 116, pp 8817-8818, 1994

[79]   Y Lvov, K Ariga, M Onda, I Ichinose, T Kunitake "A careful examination of the adsorption step in the alternate layer-by-layer assembly of linear polyanion and polycation," *Colloid Surf A Physicochem Eng Asp*, vol 146, pp 337-346, 1999

[80]   N Fujii, K Fujimoto, T Michinobu, M Akada, J P Hill, S Shiratori, K Ariga, K Shigehara "The simplest layer-by-layer assembly structure Best paired polymer electrolytes with one charge per main chain carbon atom for multilayered thin films," *Macromolecules*, vol 43, pp 3947-3955, 2010

[81]   Y Lvov, K Ariga, T Kunitake "Layer-by-layer assembly of alternate protein/polyion ultrathin films," *Chem Lett*, vol 23, pp 2323-2326, 1994

[82]   Y Lvov, K Ariga, I Ichinose, T Kunitake "Assembly of multicomponent protein films by means of electrostatic layer-by-layer adsorption," *J Am Chem Soc*, vol 117, pp 6117-6123, 1995

[83]   F Caruso, D N Furlong, K Ariga, I Ichinose, T Kunitake "Characterization of polyelectrolyte-protein multilayer films by atomic force microscopy, scanning electron microscopy, and fourier transform infrared reflection-absorption spectroscopy," *Langmuir*, vol 14, pp 4559-4565, 1998

[84]   Y Lvov, M Onda, K Ariga, T Kunitake "Ultrathin films of charged polysaccharides assembled alternately with linear polyions," *J Biomater Sci Polym Edi*, vol 9, pp 345-355, 1998

[85]   Y Lvov, K Ariga, I Ichinose, T Kunitake "Formation of ultrathin multilayer and hydrated gel from montmorillonite and linear polycations," *Langmuir*, vol 12, pp 3038-3044, 1996

[86]   Y Lvov, K Ariga, M Onda, I Ichinose, T Kunitake "Alternate assembly of ordered multilayers of SiO$_2$ and other nanoparticles and polyions," *Langmuir*, vol 13, pp 6195-6203, 1997

[87]   K Ariga, Y Lvov, I Ichinose, T Kunitake "Ultrathin films of inorganic materials (SiO2 nanoparticle, montmorillonite microplate, and molybdenum oxide) prepared by alternate layer-by-layer assembly with organic polyions," *App Clay Sci*, vol 15, pp 137-152, 1999

[88]   K Ariga, Y Lvov, T Kunitake "Assembling alternate dye-polyion molecular films by electrostatic layer-by-layer adsorption," *J Am Chem Soc*, vol 119, pp 2224-2231, 1997

[89]   K Katagiri, R Hamasaki, K Ariga, J Kikuchi "Layered paving of vesicular nanoparticles formed with cerasome as a bioinspired organic-inorganic hybrid," *J Am Chem Soc*, vol 124, pp 7892-7893, 2002

[90]   K Katagiri, R Hamasaki, K Ariga, J Kikuchi "Layer-by-layer self-assembling of liposomal nanohybrid 'cerasome' on substrates," *Langmuir*, vol 18, pp 6709-6711, 2002

[91]   H Lee, L J Kepley, H G Hong, T E Mallouk "Inorganic analogs of Langmuir-Blodgett films Adsorption of orderd zirconium 1,10-decanebisphosphonate multilayers on silicon surfaces," *J Am Chem Soc*, vol 110, pp 618-620, 1988

[92]   M Wanunu, A Vaskevich, S R Cohen, H Cohen, R Arad-Yellin, A Shanzer, I Rubinstein "Branched coordination multilayers on gold," *J Am Chem Soc*, vol 127, pp 17877-17887, 2005

[93]   W B Stockton, M F Rubner "Molecular-level processing of conjugated polymers 4 Layer-by-layer manipulation of polyaniline via hydrogen-bonding interactions," *Macromolecules*, vol 30, pp 2717-2725, 1997

[94]   S A Sukhishvili, S Granick "Layered, erasable, ultrathin polymer films," *J Am Chem Soc* , vol 122, pp 9550-9551, 2000

[95]   J Chen, L Huang, L Ying, G Luo, X Zhao, W Cao "Self-assembly ultrathin films based on diazoresins," *Langmuir*, vol 15, pp 7208-7212, 1999

[96]   G K Such, J F Quinn, A Quinn, E Tjipto, F Caruso "Assembly of ultrathin polymer multilayer films by click chemistry," *J Am Chem Soc* , vol 128, pp 9318-9319, 2006

[97]   A Ikeda, T Hatano, S Shinkai, T Akiyama and S Yamada "Efficient photocurrent generation in novel self-assembled multilayers comprised of 60]fullerene-cationic homooxacalix arene inclusion complex and anionic porphyrin polymer," *J Am Chem Soc* , vol 123, pp 4855-4856, 2001

[98]   Y Lvov, K Ariga, I Ichinose, T Kunitake "Layer-by-layer architectures of concanavalin A by means of electrostatic and biospecific interactions," *J Chem Soc Chem Commun* , pp 2313-2314, 1995

[99]   T Hoshi, S Akase, J Anzai "Preparation of multilayer thin films containing avidin through sugar-lectin interactions and their binding properties," *Langmuir*, vol 18, pp 7024-7028, 2002

[100]   Y Shimazaki, M Mitsuishi, S Ito, M Yamamoto "Preparation and characterization of the layer-by-layer deposited ultrathin film based on the charge-transfer interaction in organic solvents," *Langmuir*, vol 14, pp 2768-2773, 1998

[101]   T Serizawa, K Hamada, T Kitayama, N Fujimoto, K Hatada, M Akashi "Stepwise stereocomplex assembly of stereoregular poly(methyl methacrylate)s on a substrate," *J Am Chem Soc*, vol 122, pp 1891-1899, 2000

[102]   T Serizawa, K Hamada, M Akashi "Polymerization within a molecular-scale stereoregular template," *Nature*, vol 429, pp 52-55, 2004

[103]   S -S Lee, J -D Hong, C H Kim, K Kim, J P Koo, K -B Lee "Layer-by-layer deposited multilayer assemblies of ionene-type polyelectrolytes based on the spin-coating method," *Macromolecules*, vol 34, pp 5358-5360, 2001

[104]   C J Lefaux, J A Zimberlin, A V Dobrynin, P T Mather "Polyelectrolyte spin assembly Influence of ionic strength on the growth of multilayered thin films," *J Polym Sci B*, vol 42, pp 3654-3666, 2004

[105]   A Izquierdo, S S Ono, J -C Voegel, P Schaaf, G Decher "Dipping versus spraying Exploring the deposition conditions for speeding up layer-by-layer assembly," *Langmuir*, vol 21, pp 7558-7567, 2005

[106]   S S Shiratori, T Ito, T Yamada "Automatic film formation system for ultra-thin organic/inorganic hetero-structure by mass-controlled layer-by-layer sequential adsorption method with 'nm' scale accuracy," *Colloids Surf A*, vol 198, pp 415-423, 2002

[107]   S L Clark, P T Hammond "Engineering the microfabrication of layer-by-layer thin films," *Adv Mater*, vol 10, pp 1515-1519, 1998

[108]   Y Okahata, T Tsuruta, K Ijiro, K Ariga "Langmuir-Blodgett films of an enzyme-lipid complex for sensor membranes," *Langmuir*, vol 4, pp 1373-1375, 1988

[109]   Y Okahata, T Tsuruta, K Ijiro, K Ariga "Preparations of Langmuir-Blodgett films of enzyme-lipid complexes A glucose sensor membrane," *Thin Solid Films*, vol 180, pp 65-72, 1989

[110]   M Onda, Y Lvov, K Ariga, T Kunitake "Sequential actions of glucose oxidase and peroxidase in molecular films assembled by layer-by-layer alternate adsorption," *Biotechnol Bioeng*, vol 51, pp 163-167, 1996

[111]   M Onda, Y Lvov, K Ariga, T Kunitake "Sequential reaction and product separation on molecular films of glucoamylase and glucose oxidase assembled on an ultrafilter," *J Ferment Bioeng*, vol 82, pp 502-506, 1996

[112]   M Onda, K Ariga, T Kunitake "Activity and stability of glucose oxidase in molecular films assembled alternately with polyions," *J Biosci Bioeng*, vol 87, pp 69-75, 1999

[113]   G Sukhorukov, E Donath, S Davis, H Lichtenfeld, F Caruso, V Popov, H Mohwald "Step-wise polyelectrolyte assembly on particle surfaces-a novel approach to colloid design," *Polym Adv Technol*, vol 9, pp 759, 1998

[114]   F Caruso, R A Caruso, H Mohwald "Nanoengineering of inorganic and hybrid hollow spheres by colloidal templating," *Science*, vol 282, pp 1111-1114, 1998

[115]   G Sukhorukov, M Brumen, E Donath, H Mohwald "Hollow polyelectrolyte shells Exclusion of polymers and Donnan equilibrium," *J Phys Chem B*, vol 103, pp 6434-6440, 1999

[116] A Antipov, G Sukhorukov, E Donath, H Mohwald "Sustained release properties of polyelectrolyte multilayer capsules," *J Phys Chem B*, vol 105, pp 2281-2284, 2001

[117] X Qiu, S Leporatti, E Donath, H Mohwald "Studies on the drug release properties of polysaccharide multilayers encapsulated ibuprofen microparticles," *Langmuir*, vol 17, pp 5375-5380, 2001

[118] Y Lvov, A Antipov, A Mamedov, H Mohwald, G Sukhorukov "Urease encapsulation in nanoorganized microshells," *Nano Letters*, vol 1, pp 125-128, 2001

[119] G Sukhorukov "Multilayer hollow microspheres," *Multilayer Hollow Microspheres MML Series*, vol 5, pp 111-147, 2002

[120] B De Geest,N Sanders,G Sukhorukov, J Demeestera , S Smedt "Release mechanisms for polyelectrolyte capsules," *Chem Soc Rev* , vol 36, pp 636-649, 2007

[121] B D Geest, G Sukhorukov, H Mohwald "The pros and cons of polyelectrolyte capsules in drug delivery," *Expert Opinions Drug Deliv* , vol 6, pp 613-624, 2009

[122] L J Cock, S Koker, B G Geest, J Grooten, C Vervaet, J P Remon, G B Sukhorukov, M N Antipina "Polymeric multilayer capsules in drug delivery," *Angewandte Chemie Inter Ed* , vol 49, pp 6954-6973, 2010

[123] H Ai, S Jones, M de Villiers, Y Lvov "Nanoencapsulation of furosemide microcrystals for controlled drug release," *J Controlled Release*, vol 86, pp 59-66, 2003

[124]   D G Shchukin, A A Patel, G B Sukhorukov, Y M Lvov "Nanoassembly of biodegradable microcapsules for DNA encasing," *J Am Chem Soc*, vol 126, pp 3374-3375, 2004

[125]   Q He, Y Cui, J Li "Molecular assembly and application of biomimetic microcapsules," *Chem Soc Rev*, vol 38, pp 2292-2303, 2009

[126]   K Ariga, Q Ji, J P Hill "Enzyme-encapsulated layer-by-layer assemblies Current Status and challenges toward ultimate nanodevices," *Adv Polym Sci*, vol 229, pp 51-87, 2010

[127]   L L del Mercato, P Rivera-Gil, A Z Abbasi, M Ochs, C Ganas, I Zins, C Soennichsen, W J Parak "LbL multilayer capsule Recent progress and future outlook for their use in life sciences," *Nanoscale*, vol 2, pp 458-467, 2010

[128]   K N Anil Kumar, S Basu Ray, V Nagaraja, A M Raichur "Encapsulation and release of rifampicin using poly(vinyl pyrrolidone)-poly(methacrylic acid) polyelectrolyte capsules," *Mater Sci Eng C*, vol 29, pp 2508-2513, 2009

[129]   Q Zhao, B Han, Z Wang, C Gao, C Peng, J Shen "Hollow chitosan-alginate multilayer microcapsules as drug delivery vehicle Doxorubicin loading and in vitro and in vivo studies," *Nanomed Nanotechnol Biol Med*, vol 3, pp 63-74, 2007

[130]   Y Chen, X Lin, H Park, R Greever "Study of artemisinin nanocapsules as anticancer drug delivery systems," *Nanomed Nanotechnol Biol Med*, vol 5, pp 316-322, 2009

[131]   J Liu, Y Zhang, C Wang, R Xu, Z Chen, N Gu "Magnetically sensitive alginate-templated polyelectrolyte multilayer microcapsules for controlled release of doxorubicin," *J Phys Chem C*, vol 114, pp 7673-7679, 2010

[132]   H Y Koo, H -J Lee, J K Kim, W S Choi "UV-triggered encapsulation and release from polyelectrolyte microcapsules decorated with photoacid generators," *J Mater Chem*, vol 20, pp 3932-3937, 2010

[133]   S Shu, C Sun, X Zhang, Z Wu, Z Wang, C Li "Hollow and degradable polyelectrolyte nanocapsules for protein drug delivery," *Acta Biomater*, vol 6, pp 210-217, 2010

[134]   P Rivera-Gil, S De Koker, B G De Geest, W J Parak "Mediated by biodegradable polyelectrolyte capsules," *Nano Lett*, vol 9, pp 4398-4402, 2009

[135]   Y Itoh, M Matsusaki, T Kida, M Akashi "Enzyme-responsive release of encapsulated proteins from biodegradable hollow capsules," *Biomacromolecules*, vol 7, pp 2715-2718, 2006

[136]   Y Ma, W F Dong, M A Hempenius, H Mohwald, J Vancso "Redox-controlled molecular permeability of composite-wall microcapsules," *Nat Mater*, vol 5, pp 726-729, 2006

[137]   A L Becker, A N Zelikin, A P R Johnston, F Caruso "Tuning the formation and degradation of layer-by-layer assembled polymer hydrogel microcapsules," *Langmuir*, vol 25, pp 14079-14085, 2009

[138]   S F Chong, A Sexton, R De Rose, S J Kent, A N Zelikin, F Caruso "A paradigm for peptide vaccine delivery using viral epitopes encapsulated in degradable polymer hydrogel capsules," *Biomaterials*, vol 30, pp 5178-5186, 2009

[139]   T Addison, O J Cayre, S Biggs, S P Armes, D York "Polymeric microcapsules assembled from a cationic/zwitterionic pair of responsive block copolymer micelles," *Langmuir*, vol 26, pp 6281-6286, 2010

[140]   X Li, T Lu, J Zhang, J Xu, Q Hu, S Zhao, J Shen "A study of properties of 'micelle-enhanced' polyelectrolyte capsules Structure, encapsulation and in vitro release," *Acta Biomater* , vol 5, pp 2122-2131, 2009

[141]   F Cavalieri, A Postma, L Lee, F Caruso "Assembly and functionalization of DNA-polymer microcapsules," *ACS Nano*, vol 3, pp 234-240, 2009

[142]   Y Fukui, K Fujimoto "The preparation of sugar polymer-coated nanocapsules by the layer-by-layer deposition on the liposome," *Langmuir*, vol 25, pp 10020-10025, 2009

[143]   Z S Haidar, R C Hamdy, M Tabrizian "Biocompatibility and safety of a hybrid core-shell nanoparticulate OP-1 delivery system intramuscularly administered in rats," *Biomaterials*, vol 31, pp 2746-2754, 2010

[144]   J F P da Silva Gomes, A Rank, A Kronenberger, J Fritz, M Winterhalter, Y Ramaye "Polyelectrolyte-coated unilamellar nanometer-sized magnetic liposomes," *Langmuir*, vol 25, pp 6793-6799, 2009

[145]   B G De Geest, S De Koker, K Immesoete, J Demeester, S C De Smedt, W E Hennink "Self-exploding beads releasing microcarriers," *Adv Mater* , vol 20, pp 3687-3691, 2008

[146]   J Bai, S Beyer,   W C Makd,   D Trau   "Fabrication of   inflated LbL microcapsules with a 'bead-in-a-capsule' morphology," *Soft Matter*, vol 5, pp 4152-4160, 2009

[147]   H Ke, Z Xing, B Zhao, J Wang, J Liu, C Guo1, Xiuli Yue, S Liu, Z Tang, Z Dai "Quantum-dot-modified microbubbles with bi-mode imaging capabilities," *Nanotechnolog*, vol 20, pp 425105, 2009

[148]   P Pattekari, Z Zheng, X Zhang, T Levchenko, V Torchiln, Y Lvov "Top-down and bottom-up approach in production aqueous nanocolloids of paclitaxel," *Phys Chem Chem Phys* , vol 13, pp 1624-1629, 2011

[149]   Z Zheng, X Zhang, D Carbo, C Clark, C-A Nathan, Y Lvov "Sonication assisted synthesis of polyelectrolyte coated curcumin nanoparticles," *Langmuir*, vol 26, pp 7679-7681, 2010

[150]   J Cui, B Yu, Y Zhao, W Zhu, H Li, H Lou, G Zhai "Enhancement of oral absorption of curcumin by self-microemulsifying drug delivery systems," *Int J of Pharmaceutics*, vol 371, pp 148-155, 2009

[151]   V Belova,   D Gorin,   D Shchukin,   H Mohwald   "Selective ultrasonic cavitation at patterned hydrophobic surfaces," *Angewandte Chemie Inter Ed* , vol 122, pp 7129-7134, 2010